Phase Equilibria and Thermodynamic Properties of High-Alloy Tool Steels

Theoretical and Experimental Approach

Johan Bratberg

Doctoral Thesis

Stockholm, Sweden 2005

Department of Material Science and Engineering
Division of Physical Metallurgy
Royal Institute of Technology
Brinellvägen 23
100 44 Stockholm, Sweden
and
Corrosion and Metals Research Institute
Computational Thermodynamics Research Group
Drottning Kristinas väg 48
114 28 Stockholm, Sweden

ISRN KTH/MSE--05/62--SE+METO/AVH
ISBN 91-7178-120-X

Akademisk avhandling som med tillstånd av Kungliga Tekniska Högskolan i Stockholm framlägges till offentlig granskning för avläggande av teknologie doktorsexamen fredagen den 21:a oktober 2005 kl. 10.00 i Salongen, KTHB, Osquars backe 31, Stockholm. Fakultetsopponenten är Dr. Bengt Hallstedt, Lehrstuhl für Werkstoffchemie, Materials Chemistry, Aachen, Germany.

© Johan Bratberg, september 2005

Tryck: Universitetsservice US AB, www.us-ab.com

Phase Equilibria and Thermodynamic Properties of High-Alloy Tool Steels - Theoretical and Experimental Approach

Johan Bratberg

Abstract

The recent development of tool steels and high-speed steels has led to a significant increase in alloy additions, such as Co, Cr, Mo, N, V, and W. Knowledge about the phase relations in these multicomponent alloys, that is, the relative stability between different carbides or the solubility of different elements in the carbides and in the matrix phase, is essential for understanding the behaviour of these alloys in heat treatments. This information is also the basis for improving the properties or designing new alloys by controlling the amount of alloying elements. Thermodynamic calculations together with a thermodynamic database is a very powerful and important tool for alloy development of new tool steels and high-speed steels. By thermodynamic calculations one can easily predict how different amounts of alloying elements influence on the stability of different phases. Phase fractions of the individual phases and the solubility of different elements in the phases can be predicted quickly. Thermodynamic calculations can also be used to find optimised processing temperatures, e.g. for different heat treatments. Combining thermodynamic calculations with kinetic modelling one can also predict the microstructure evolution in different processes such as solidification, dissolution heat treatments, carbide coarsening, and the important tempering step producing secondary carbides.

The quality of predictions based on thermodynamic calculations directly depends on the accuracy of the thermodynamic database used. In the present work new experimental phase equilibria information, both in model alloys containing few elements and in commercial alloys, has been determined and was used to evaluate and improve the thermodynamic description. This new experimental investigation was necessary because important information concerning the different carbide systems in tool steels and high-speed steels were lacking.

A new thermodynamic database for tool steels and high-speed steels, TOOL05, has been developed within this thesis. With the new database it is possible to calculate thermodynamic properties and phase equilibria with high accuracy and good reliability. Compared with the previous thermodynamic description the improvements are significant. In addition the composition range of different alloying elements, where reliable results are obtained with the new thermodynamic database, have been widened significantly.

As the available kinetic data did not always predict results in agreement with new experiments the database was modified in the present work. By coupling the new thermodynamic description with the new kinetic description accurate diffusion simulations can be performed for carbide coarsening, carbide dissolution and micro segregation during solidification.

Keywords: Thermodynamic modelling, Thermodynamic calculations, Tool Steels, High-speed Steels, CALPHAD, Phase equilibria, Phase diagram, WDS/EDS, Thermo-Calc, Carbide coarsening, Diffusion simulations, DICTRA

Preface

The research presented in this thesis was carried out at the Corrosion and Metals Research Institute (Kimab) during year 2001 until 2005 and includes an introductory part and the following appended papers, which will be referred to by the following roman numbers:

I. **Johan Bratberg and Karin Frisk**
A Thermodynamic Analysis of the Mo-V and Mo-V-C Systems
Calphad, Vol. 26, No. 3, 2002, pp. 459-476

II. **Johan Bratberg and Bo Sundman**
A Thermodynamic Assessment of the Co-V System
Journal of Phase Equilibria, Vol. 24, No. 6, 2003, pp. 495-503

III. **Johan Bratberg and Karin Frisk**
An Experimental and Theoretical Analysis of the Phase Equilibria in the Fe-Cr-V-C System
Met. Mat. Trans. A, Vol. 35A, No. 12, 2004, pp. 3649-3663

IV. **Johan Bratberg and Karin Frisk**
An Experimental Investigation of Carbide/Austenite Equilibria in Commercial Tool Steels and High-Speed Steels Compared Against Thermodynamic Calculations
Proceeding of the Powder Metallurgy World Congress and EURO-PM2004, Vienna, Vol. 5, 2004, pp. 337-342

V. **Johan Bratberg**
Investigation and Modification of Carbide Sub-Systems in the Multicomponent Fe-C-Co-Cr-Mo-Si-V-W System
Zeitschrift für Metallkunde, Vol. 96, No. 4, 2005, pp. 335-344

VI. **Johan Bratberg, John Ågren and Karin Frisk**
Diffusion Simulations of MC and M_7C_3 Carbide Coarsening in bcc and fcc Matrix Utilising a New Thermodynamic and Kinetic Description
Submitted to Materials Science and Technology, April 2005

VII. **Karin Frisk, Johan Bratberg and Andreas Markström**
Thermodynamic Modelling of the M_6C Carbide in Cemented Carbides and High-Speed Steel
Calphad, Vol. 29, No. 2, 2005, pp. 91-96

VIII. **Johan Bratberg and Karin Frisk**
An Investigation of Lower-Order N Containing Systems and New Phase Equilibria Experiments in the Fe-Cr-Mo-V-C-N System
Submitted to Zeitschrift für Metallkunde, September 2005

I have also been involved in the work resulting in the following papers during this period. However, they have been omitted due to confidential work or for being outside the scope of this thesis.

IX. **Johan Bratberg and Bo Jansson**
A Thermodynamic Evaluation of the C-Co-W-Hf-Zr System for Cemented Carbide Applications
Submitted to Journal of Phase Equilibria and Diffusion, 2005

X. **Johan Bratberg**
DICTRA Simulations on How Tungsten Influence the Sigma Phase Precipitation in Superaustenitic Stainless Steels
IM-Report-40762, Kimab, Stockholm, Sweden, 2003

XI. **Johan Bratberg and Karin Frisk**
An Experimental Investigation of Carbide/Austenite Equilibria in Commercial Tool Steel and High-Speed Steel Systems
IM-Report-2005-534, Confidental Report, Open Year 2015, Kimab, Stockholm, Sweden, 2004

Stockholm, September 2005

Johan Bratberg

Contents

1. Introduction 1

1.1 Historic Background of Tool Steels 1
1.2 Alloy Design and Influence of Alloying Elements in Tool Steels 3
1.3 Computational Thermodynamics and the CALPHAD Technique 6
1.4 Aim of this Work 8

2. Thermodynamic and Kinetic Modelling 11

2.1 Thermodynamic Models 11
2.2 Kinetic Models 16
2.3 Simulation of Coarsening and diffusion 19

3. Experimental Techniques and Methodology 23

3.1 Model Alloys Design for Critical Phase Equilibria Experiments 23
3.2 Heat Treatments to Reach Phase Equilibria 24
3.3 Analysis of Heat Treated Samples 24
  3.3.1 SEM Using Backscattered Electron Detector 24
  3.3.2 WDS/EDS Measurements with ASEM 25
  3.3.3 Electron Microprobe Analysis 29
  3.3.4 EBSP Analysis 30
  3.3.5 MicroGOP Analysis 31
3.4 Experimental Results and Discussion 31

4. Development of a New Thermodynamic Database Utilising the new Phase Equilibria Information 35

4.1 Work Plan 35
4.2 Verification of Results Using Commercial Tool Steel Alloys 36
4.3 Status Today and Possible Applications 38

5. Coarsening Experiments and Simulations to Assess Tracer Diffusion Data 47

5.1 Assessment of Tracer Diffusion Data for Mobility Evaluation Using New Experimental Coarsening Information 47
5.2 The Influence of the Thermodynamic Description 47
5.3 The Influence of the Interfacial Energy 49

6. **Summary of Appended Papers** 51

6.1 Paper I 51
6.2 Paper II 52
6.3 Paper III 53
6.4 Paper IV 54
6.5 Paper V 55
6.6 Paper VI 56
6.7 Paper VII 57
6.8 Paper VIII 58

7. **Conclusions and Future Work** 59

7.1 Conclusions of the Work 59
7.2 Future Work and Applications 59
  7.2.1 Extend the Temperature Range 59
  7.2.2 Elements that Needs to be Evaluated and to be Added to the Present Thermodynamic Database 60
  7.2.3 Use of First-principles Calculations 60
  7.2.4 Diffusion Simulations 61

8. **Acknowledgements** 63

9. **References** 65

1. Introduction

1.1 Historic Background of Tool Steels

Iron was used in small amounts long before it was found how to smelt it. This iron was recovered from meteorites and was used as the tips of spears around 4000 BC in Ancient Egypt and Sumer. The transition from iron to steel was possibly the accidental discovery that, in the heating of meteoric iron for shaping, it absorbed carbon from contact with a carbonaceous material. The earliest uses of steel known were for tools. The formation of martensite from austenite (increases the hardness) by quenching in water is so old that the time of its discovery has never been accurately dated. The oldest quench-hardened steel artefact was found 1100 BC on Cyprus and was a knife.

The crucible technique was used to produce high quality steel in southern India perhaps as early as 300 BC. Some discussions about this date have occurred if it is to early or not but all are agreed that it certainly was produces by AD 200. Here, high-purity wrought iron, charcoal, and glass were mixed in crucibles and heated until the iron melted and absorbed the carbon. The steel from this process was high in carbon and was called Pulad in Arabic and Wootz by later Europeans. It found a large market throughout much of Asia. It appears that steelmaking by melting and solidification was also practised by the Chinese, possibly long before the manufacture of Wootz steels. The knowledge of steelmaking was after this time under a long succession of years not improved. This period is known as the dark ages.

Benjamin Huntsman from Handsworth in England rediscovered the crucible steel year 1740. Small ceramic crucibles were used in his process where wrought iron and cast iron were heated until melting together to form steel. The next major discovery in the field of tool steels after Huntsman's was that of so-called Mushet steel in 1868. Robert Mushet suggested addition of manganese in the production route of Bessemer Steel and this made the Bessemer process commercial. During this time he also became interested in different alloying elements in steel. A lot of experimental work was performed and he discovered that one of the bars of steel he had made seemed to have the property of becoming hard after heating without the usual quenching that had been used from time immemorial for hardening i.e. the steel was self hardening. The analysis of this steel bar showed it to contain significant amounts of tungsten. Mushet was not primarily interested in tool steels, but he almost immediately recognised how much such a property might be of an advantage in tool steels.

In a paper by Dr. John W. Langley, presented 1892 in the American Society of Civil Engineers [1], it was pointed out that the addition of tungsten alone to steel did not make the steel self-hardening. It was shown that high amounts of manganese or chromium were needed in steels for them to be self-hardening. Langley had used the original composition of Mushet´s self-hardening steel and just added small amounts of chromium. In a work by A. S. Townsend [2] the history of the transition from manganese-tungsten self-hardening steel to chromium-tungsten self-hardening steel was thoroughly investigated. A large experimental investigation about self-hardening steels was performed by Mr. Fred W. Taylor [3] 1898. He tried to find out which steel was best suited for particular applications. At that time steels were ruined very quickly by high temperatures, but he found that tungsten addition improved the resistance to deformation at high temperatures so greatly that cutting speeds became possible which previously had been only dreamed of. After these discoveries Taylor became associated with the red-hardness phenomena, i.e. the tool steels resistance to deformation at elevated temperature.

In 1900, Taylor and White recommended a steel containing 1.85 mass % C, 3.80 mass % Cr and 8.00 mass % W. In about 1903, they recommended a steel containing 0.70 mass % C and at least 14.00 mass % W. This alloy is the prototype of our modern high-speed steels. This great advance was called the Taylor-White process. The effect of vanadium in compositions of high-speed steels was briefly studied as early as 1900, but the price was so high at that time that investigations were not proceeded. Vanadium found its way into the composition of modern high-speed steels between 1904 and 1906, and the amount in the first commercial steels was about 0.30 mass %. This amount was slowly increased so that around 1910 high-speed steels were being generally manufactured containing about 0.70 mass %.

Between 1912 and 1920 the amount of Co increased up to 12 mass % to allow a further increase in cutting speed. Another major development around year 1939 was the discovery that carefully balanced additions of high vanadium and increased carbon would form large amounts of very hard and relative large vanadium carbides in the structure. These carbides greatly increase the abrasion resistance of the steel. After the entrance of vanadium the trend during 1940 until 1952 was to increase the substitution of molybdenum for tungsten. This alloy development resulted around year 1960 in a hardness close 70 Rockwell C after heat treatment. More detailed information about the history of iron and the development of tool steels can be found in references [4, 5].

In the last decades the development of tool steels and high-speed steels has led to a significant increase of the contents of Co, Cr, Mo, Nb, V, and W. These kinds of steel normally contain 1-3 mass % carbon and up to 25 percent phase fraction of different carbides. In some special high-speed steels aluminium is also added up to 1 mass %. The latest trend is to increase the nitrogen amount in the alloys to form carbonitrides instead of MC carbides. Nitrogen amounts up to 3 mass % are used and the nitrogen substitutes the carbon in the MC carbides and carbonitrides are formed, which changes the distribution of different carbide formers.

In addition to this alloy development, a number of special heat treating procedures, like carburising, nitriding, refrigeration, and bainitic hardening have been applied to tool steels and high-speed steels in the last decades. At the same time the steel making and processing procedures have also been refined and heat treatment has been optimised and made much more precise. The phase composition of the final product, which largely determines its properties, critically depends on the manufactory technique and solidification conditions.

1.2 Alloy Design and Influence of Alloying Elements in Tool Steels

Tool steel refers to a rather wide variety of carbon and alloy steels that are particularly well-suited as tool materials. Their suitability comes from their distinct toughness, resistance to abrasion, their ability to hold a cutting edge and/or their resistance to deformation at elevated temperature (red-hardness). It includes steels suitable for various types of cutting tools, press tools, hot and cold heading dies, moulds for plastics and die- casting, extrusion tools, hand tools, etc.

When tool steels contain a combination of more than 7 mass % tungsten, together with molybdenum and vanadium, along with more than 0.60 mass % carbon, they are referred to as high-speed steels. The term high-speed steel was derived from the fact that it is capable of cutting metal at a much higher rate than plain carbon tool steel and continues to cut and retain its hardness even when the point of the tool is heated to a low red temperature. Tungsten is the major alloying element but it is also combined with molybdenum, vanadium and cobalt in varying amounts. Although replaced by cemented carbides for many applications it is still widely used for the manufacture of taps, dies, twist drills, reamers, saw blades and other cutting tools.

It is not possible maximise fracture toughness and yield strength simultaneously. A property compromise must be found, taking into account the service conditions as well as aspects of production and economics. Every application for tool steels and high-speed steels is unique, so for every specific case one must optimise the properties as toughness, wear-resistance, grindability, machinability, dimensional stability, and heat resistance. All of these characteristics combine to create the true value of tool steels, as it is defined in terms of a tool's performance or life.

All the above properties are strongly related to the microstructure, which depends on the alloying elements and the manufacturing process route. The basic feature of the microstructure in tool steels and high-speed steels is the high volume fraction of carbides, up to 25 percent phase fraction (volume fraction). It has been known that the performance and service life of tool steels and high-speed steels are closely related to the composition, phase structure, size, morphology, and distribution of carbides in the alloy. The microstructure of tool steels and high-speed steels after tempering consist of a combination of primary MC, M_7C_3, and M_6C carbides and a fine dispersion of MC and M_2C type carbides, the last ones precipitate during the tempering process. The fine dispersion carbides are responsible for the secondary hardening and are therefore called secondary carbides, although in the sequence of phase formation they belong to a later generation. Use at high temperatures will cause further precipitation of fine dispersed carbides, and eventually deteriorate the strength due to growth of the secondary carbides, overtempering. A highly tempered martensitic matrix surrounds the coarse, blocky primary carbides. Before tempering it is supersaturated with carbide forming elements. A large amount of alloy elements, about 15 to 35 mass %, must be intentionally added to iron in order to obtain this microstructure. As mentioned the usual additions besides carbon are chromium, vanadium, molybdenum, cobalt, niobium, nitrogen, tungsten, and sometimes also aluminium. Furthermore, small amounts of Si, Mn and Ni and other elements, whose total amount usually does not exceed 1 mass %, are also present in these alloys. Below follows a brief description on the role of the different alloying elements.

Carbon, the essential element in carbides is added in specific amounts for formation of primary and secondary carbides that control the hardness and strength. In general, increased carbon content reduces ductility but increases tensile strength and the ability of the steel to harden when cooled rapidly from elevated temperatures.

Molybdenum promotes high hardness and wear resistance at high temperatures. A large amount of molybdenum dissolves in the M_6C carbide and in more modest amounts in the MC carbide. In a study by Fischmeister et al. [6] it was shown that molybdenum favours the solidification of the eutectic via M_2C, creating a finer eutectic structure compared to M_6C. During hot working, the M_2C decomposes into M_6C and MC [7, 8], and will not be present in the final microstructure of most high-speed steels.

Chromium increases the hardenability and in combination with high carbon it gives resistance to wear and abrasion. Chromium has an important effect on corrosion resistance and has a high solubility in the M_7C_3 carbide. Finally, chromium is one of the major metallic constituents of the secondary carbides and plays an important role in nucleation of the secondary precipitates responsible for the high hardness at high temperature [9].

Cobalt does not act as a carbide former, although amounts up to 5 mass % in the M_6C carbide has been reported [10], but goes mostly to the matrix, promoting solid solution strengthening. Together with tungsten and molybdenum, cobalt is used to form the super high-speed steels. It improves the red hardness value of the high-speed steel, that is, it enables the steel to resist softening at a high temperature or in the case of a cutting tool to hold its edge under severe conditions. Cobalt is also claimed to improve the precipitation of secondary carbides, and to retard their growth [11].

Vanadium combines with carbon and nitrogen to precipitate in the form of hard, isolated carbides and carbonitrides, which are important in promoting abrasion resistance. The solubility of vanadium in MC carbides and carbonitrides is high. Vanadium also raises the temperature at which grain coarsening sets in and increases hardenability, where it is in solution in the austenite prior to quenching. It also reduces softening on tempering and confers secondary hardness on high-speed steels. Together with Mo and Cr, vanadium is one of the elements mainly involved in the secondary precipitation reaction [9].

Tungsten has a similar effect as molybdenum, by promoting high hardness and wear resistance at high temperatures. Its "red hardness" value makes it suitable for cutting tools as it enables the tool edge to be maintained at high temperatures. In conjunction with other alloying elements it finds applications at high temperatures and other severe service conditions. Tungsten has a large solubility in the M_6C carbide, but also a relatively high solubility in the MC carbide.

Niobium is a very strong carbide former, even stronger than vanadium, and its monocarbide does not dissolve much of other elements at high temperatures. In a work by Karagöz and Fischmeister [12] it is described how this behaviour could be used to generate stable primary carbides and to make the secondary carbides compositionally independent from the primary. The maximum niobium additions are however limited to about 2 mass % using conventional metallurgy and casting, because of the tendency of the MC carbides to grow very large [13], but processing via the powder metallurgy route allows the use of higher niobium levels [14].

Nitrogen can combine with many metals to form nitrides and is thus applied to case-hardening of steel, the usual source for this purpose being ammonia. Nitrogen atoms substitute carbon atoms and form very hard carbonitrides. This phenomenon also affects the distribution of carbide forming elements.

Manganese is one of the most important constituents of steel in which it fulfils a number of functions. It acts as a mild de-oxidising agent. It combines with the sulphur present to form globular inclusions of Manganese Sulphide which are beneficial to machining. It increases tensile strength and the hardenability of steel.

Silicon is used up to 1 mass % in tool steels and high-speed steels. The presence of silicon increases the structural strength due to solid solution strengthening. Silicon also promotes the formation of M_6C carbide [15] and an increased silicon content will also increase the carbon activity in a multicomponent alloy. Silicon is also a strong ferrite stabiliser and is used as a de-oxidising element.

Aluminium is like silicon a strong ferrite stabiliser, much stronger than silicon in fact. Aluminium's large oxygen affinity makes it a good de-oxidising element.

1.3 Computational Thermodynamics and the CALPHAD Technique

Computational thermodynamics is an important and powerful tool in the development process of new tool steels and high-speed steels. The Thermo-Calc software [16] uses Gibbs energy expressions stored in databases. Each phase, in a given system, is represented by a Gibbs energy expression, i.e. a function of composition, pressure, and temperature. When calculating different thermodynamic properties the software uses 1:st and 2:nd derivatives of the Gibbs energy expressions to the minimum that represents the equilibrium state. Such calculations can significantly decrease the number of experiments needed for the development of a new alloy. One can easily quantify how different amounts of alloying elements influence the stability of different kinds of carbides. Also phase fractions of the carbides and solubility of different elements in the carbides can be calculated quickly. Computational thermodynamics may also be used to optimise temperatures for heat treatment. All kind of thermodynamic properties may be calculated, e.g. enthalpy of formation, heat capacity, Gibbs energies etc. The experimental determination of phase diagrams is a time consuming and costly task. This becomes even more pronounced as the number of components increases. The thermodynamic calculations of phase diagrams reduce the effort required to determine the equilibrium constitution in a multicomponent system.

The quality of the predictions based on calculations depends on the quality of the thermodynamic databases. Several thermodynamic databases are today available and make it possible to perform equilibrium calculations in a large number of multicomponent systems. Commercial materials often contain 8-10 alloying element and through extrapolation, it is often possible to predict phase equilibria with sufficient accuracy. The use of this technique to solve industrially relevant problems increases and requires improved data reliability. To meet these increased demands available data must be adjusted. Thermodynamic data are often extrapolated from binary or ternary and higher-order systems and their validity in multicomponent alloys is rarely critically evaluated. The purpose with the evaluation of lower-order systems has often been to describe the whole range of composition with satisfactory accuracy. Compromises have thus been done without taking into account that certain parts of the phase diagrams are more technically relevant and would require much higher accuracy. Shortcomings in the thermodynamic databases may also be the result of the lack of experimental information.

This kind of thermodynamic computations are performed using the so-called CALPHAD [17, 18] technique (CALculation of PHAse Diagrams). The idea is to use models, based on physical concepts, which give simple mathematical expressions describing the Gibbs energy as a function of composition, pressure, and temperature. Available thermochemical experimental information, as well as phase diagram information, is used to fit the model parameters describing the Gibbs energy of individual phases. The objective of the CALPHAD technique is to obtain a consistent set of model parameters that can realistically describe all thermodynamic properties in a selected system.

The thermodynamic parameters are evaluated using the PARROT module [19] in the Thermo-Calc software package [16]. This module works by minimizing an error sum where each piece of information is given a certain weight according to its estimated accuracy and allows the simultaneous consideration of various types of thermodynamic and phase diagram data. The best-fit criterion follows the maximum likelihood principle and that principle as a criterion for best fit is most efficient when the amount of data is large. While modern developments in modelling and computational technology have made thermodynamic calculations of multicomponent phase equilibria a realistic possibility today, the correlation between thermodynamics and phase equilibria was established more than a century ago by J. W. Gibbs [20, 21]. A summary of the ground breaking work of Gibbs has been presented by Hertz [22].

The roots of the CALPHAD technique approach lie with van Laar [23], who applied Gibbs energy concepts to phase equilibria early in the century. To describe the solution phases van Laar used concentration dependent terms which

Hildebrand [24] later called regular solutions. The next major step in the development process was when Meijering published his calculations of miscibility gaps in ternary [25] and quaternary [26] solutions. Shortly afterwards Meijering applied this method to the thermodynamic evaluation of the Cr-Cu-Ni system [27]. Simultaneously Kaufman and Cohen [28] applied thermodynamic calculations in the analysis of the martensitic transformation in the Fe-Ni system. In parallel to Kaufman and co-workers in the USA, work was taking place in Sweden stemming from the appointment of Hillert to the Royal Institute of Technology in Stockholm 1961. Kaufman and Hillert both did their PhD studies at MIT and Hillert made the use of thermodynamic calculations a key feature of the department in Stockholm. There was also considerable encouragement from both the government and the steel making industry for such a programme of work.

The foundation of the CALPHAD method was laid in 1970 by Kaufman and Bernstein [17] who summarized the general features of the calculations of phase diagrams. In the late 1970s the extension by Sundman and Ågren [29] of the two-sublattice model of Hillert and Staffansson [30] into a general model which could account for multiple sublattices and multicomponent alloys was being undertaken. As one of the key papers on general modelling, this laid the foundation for a substantial proportion of the CALPHAD assessments that have been made to date. A continuous development of the models and the software's have since then been running. In recent years the expression ''computational thermodynamics'' is frequently used in place of ''calculations of phase diagrams''. This reflects the fact that the phase diagram is only a portion of the information that can be obtained from thermodynamic calculations.

1.4 Aim of this Work

Computational thermodynamics utilising the Thermo-Calc software [16] with the TCFE3 [31] database all show the same tendency, the calculated distribution of the alloying elements between the matrix and the carbides in commercial alloys does not agree very well with experimental information. Also the calculated relative phase stability shows large deviations compared to experimental measurements. Experience has shown that in commercial materials the amount of M_7C_3 carbide, high in chromium, is strongly underestimated and in many cases not predicted at all using the previously mentioned database. A detailed study on the interaction between chromium and vanadium was needed and adjustments of the database are accordingly needed. This kind of work also includes other elements that dissolve in significant amounts in the different carbides as Co, Mo, Si, and W.

The development of tool steels and high-speed steels has in the last decade led to a significant increase of the N amount in the alloys. Most of the nitrogen forms carbonitrides and therefore change the element distribution dramatically when going from MC carbide to a carbonitride. This behaviour has not been described thermodynamically in a satisfactory way before and is very important in the design of new alloys with high amounts of nitrogen. Therefore, an investigation and modification of important nitrogen sub-systems was motivated in the present work.

The aim of the present work was to identify the areas where predictions deviate from experimental information, to clarify the reasons for such deviations and if necessary, to improve the thermodynamic description of the alloy system under consideration. The work was limited to identify the accuracy of the thermodynamic description of the alloy system Fe, Mn, Si, Cr, Mo, V, W, Co, C, N in a composition and temperature range relevant to tool steels and high-speed steels. A further aim was to improve the thermodynamic database description and verify the results.

The final aim was to apply the thermodynamic database to solve industrial relevant problems. This could be everything from alloy development questions (solubilities, fractions, influence of different elements, etc.) to process optimising questions (temperatures, carbide dissolution, carbide coarsening, etc.). To be able to solve the latter problems a modification of the previous kinetic description was needed. Some examples on how computational thermodynamics can be a useful tool in an industrial point of view are shown in section 4.3.

2. Thermodynamic and Kinetic Modelling

2.1 Thermodynamic Models

The predictive capacity of the CALPHAD technique [17, 18] in interpolation or extrapolation to compositions and temperatures not available to experimental study and in extrapolation to higher-order systems, where full experimental information is not practically feasible, depends critically on the quality of the models used. The Gibbs energy of the liquid phase is in this thesis described by adopting a substitutional solution model [32]. All the interaction parameters in this model are in general composition dependent according to the Redlich-Kister [33] phenomenological polynomial. The interaction parameters are usually temperature dependent.

The solid phases were described by the compound energy formalism [34]. This formalism utilises different amount of sublattices and can be used to describe all relevant phases included in tool steels and high-speed steels. Eight different phases occur in these alloys, fcc(austenite), bcc(ferrite), hcp(M_2C), MC, carbonitride, M_7C_3, M_6C, and $M_{23}C_6$. The first five phases were described with a two-sublattice version of the compound energy formalism [34], $(Co,Cr,Fe,Mn,Mo,Si,V,W)_a(C,N,Va)_c$, where Va denotes vacancies. The symbols a and c are used to denote the numbers of sites on each sublattice. In the case of fcc, MC, and carbonitride, $a = c = 1$; for bcc, $a = 1$ and $c = 3$. The hcp phase is closed-packed hexagonal, yielding one octahedral interstitial site per atom. However, it was assumed that two neighbouring interstitial sites in the hexagonal c direction are never simultaneously occupied, and the maximum carbon content is thus represented by the formula M_2C. Therefore, this phase is approximated with $a = 1$ and $c = 0.5$. The Gibbs energy, for one mole of formula unit, as a function of temperature and composition is described by the expression

$$G_m^\phi = \sum_M \sum_I y_M y_I \, {}^\circ G_{M:I}^\phi + RT(a\sum_M y_M \ln y_M + c\sum_I y_I \ln y_I) + {}^E G_m^\phi + G_m^{\phi\,mg} \tag{1}$$

where M represents the elements on the first sublattice and I the elements on the second sublattice. The y parameters denote the fraction of lattice sites occupied by a given component. The quantity ${}^\circ G_{M:I}^\phi$ represents the Gibbs energy of the real or hypothetical compound $M_a I_c$ relative the so-called stable element reference (SER), which is defined as the stable state of the elements at 298.15 K and 0.1 MPa. The parameter ${}^\circ G_{M:Va}^\phi$ is the Gibbs energy of pure element M $(M = Co,Cr,Fe,Mn,Mo,Si,V,W)$ with the structure ϕ in a hypothetical non-magnetic state, and ${}^{\circ}G^{\phi}_{M:C}$ is the Gibbs energy of a hypothetical non-magnetic state where all the interstitial sites are filled with carbon atoms. In the same way the parameter ${}^{\circ}G^{\phi}_{M:N}$ is the Gibbs energy of a hypothetical non-magnetic state where all interstitial sites are filled with nitrogen atoms.

The M_7C_3 carbide was modelled with two sublattices with occupation ratio 7:3 and considered as stoichiometric with respect to carbon. The M_6C carbide was modelled in the same way but with four different sublattices with occupation ratio 2:2:2:1. The metallic sites are divided into three separate sublattices based on crystallographic information [35]. Andersson [36] suggested that the $M_{23}C_6$ carbide can be described using a three sublattices version of the compound energy formalism [34] with the occupation ratio 20:3:6, and this model was also used here.

The term ${}^{E}G^{\phi}_{m}$ in Equation (1) represents the so-called excess Gibbs energy and represents the non-ideal contribution to mixing. This expression contains interaction parameters which can be composition and temperature dependent. The composition dependence of the interaction parameters is commonly expressed by the so-called Redlich-Kister polynomial [33].

The term, $G^{\phi^{mg}}_{m}$ in Equation (1), describes the magnetic contribution to the Gibbs energy. The magnetic contribution was first described in terms of a magnetic heat capacity by Inden [37] and later Hillert and Jarl [38] integrated this heat capacity to a Gibbs energy expression.

$$G^{\phi^{mg}}_{m} = RT\ln(\beta^{\phi}+1)f(\tau) \tag{2}$$

for $\tau < 1$

$$f(\tau) = 1 - \left[\frac{79\tau^{-1}}{140p} + \frac{474}{497}\left(p^{-1}-1\right)\left(\frac{\tau^{3}}{6}+\frac{\tau^{9}}{135}+\frac{\tau^{15}}{600}\right)\right] / A \tag{3}$$

for $\tau > 1$

$$f(\tau) = -\left[\frac{\tau^{-5}}{10}+\frac{\tau^{-15}}{315}+\frac{\tau^{-25}}{1500}\right] / A \tag{4}$$

Where $A = \left(\frac{518}{1125}\right)+\left(\frac{11692}{15975}\right)\left(p^{-1}-1\right)$ and p depends on the structure given as 0.28 for fcc and hcp metals and 0.4 for bcc metals. The term β is the number of unpaired electron spins, the Bohr magneton number. It should be evaluated from the thermodynamic effect of the magnetic transition rather than from magnetic measurements. The value of τ is defined as $\tau = T / T_C$ where T_C is the Curie temperature.

Some of the adjustable parameters in the compound energy formalism [34] represent the Gibbs energy of compounds, which are not stable in the binary system. The Gibbs energy of those metastable compounds can not be measured but only be estimated. In this thesis a method developed by Fernández Guillermet and Grimvall [39] has been applied. Miedema´s formula [40] has been very successful in accounting for the enthalpy of formation of various groups of compounds, but it does not treat the entropy part of the Gibbs energy, which is important in a consideration of the phase equilibria at high temperatures. The problem of estimating Gibbs energy at high temperatures led Fernández Guillermet and Grimvall [39] to a systematic study of the thermodynamics of various 3d-transition metal compounds. Other possibilities to predict these properties are to use first-principles calculations. First-principles calculations have shown to become more and more trustful depending on the fast development of computers and improved approximations.

In the present work the estimation procedures introduced in reference [39] have been combined with the CALPHAD method [17, 18] to gain information on the thermodynamics of a metastable phase which has not been studied experimentally. The following describes how a general thermodynamic description of a metastable phase can be predicted. The Gibbs energy as a function of T per mole of formula units of a ϕ phase at 0.1 MPa, ${}^{\circ}G_m^{\phi}(T)$, is related to the molar enthalpy (${}^{\circ}H_m^{\phi}$) and the molar entropy (${}^{\circ}S_m^{\phi}$) at the reference temperature $T_0 = 298.15K$. The general Gibbs energy function, G, can be described as below,

$$G = U - TS + PV \tag{5}$$

$$dG = -SdT + VdP \tag{6}$$

from which it is seen that

$$\left(\frac{\partial G}{\partial T}\right)_P = -S \tag{7}$$

and

$$\left(\frac{\partial G}{\partial P}\right)_T = V \tag{8}$$

Equation (6) is of particular interest because T and P are the variables that are most easily controlled experimentally and they are both potentials. If both T and P are constant, then an increment of an isothermal isobaric process occurring at equilibrium requires that

$$dG = 0 \tag{9}$$

For a system undergoing a process at constant T and constant P, the Gibbs energy can only decrease or remain constant, and the attainment of equilibrium in the system coincides with the system having the minimum value of G consistent with the values of P and T.

By integrating Equation (10) we obtain an expression for the Gibbs energy for the metastable ϕ phase.

$$\left(\frac{\partial {}^{\circ}G_m^{\phi}}{\partial T}\right)_P = -{}^{\circ}S_m^{\phi} \tag{10}$$

$${}^{\circ}G_m^{\phi}(T) = {}^{\circ}H_m^{\phi}(T_0) - T_0\,{}^{\circ}S_m^{\phi}(T_0) - \int_{T_0}^{T} {}^{\circ}S_m^{\phi}(T')dT' \tag{11}$$

A value on Gibbs energy is always given relative a reference state. Using the convention adopted by the SGTE (Scientific Group Thermodata Europe) organization [41] we refer the ${}^{\circ}G_m^{\phi}(T)$ function in Equation (11) to the weighted sum of the enthalpies of the elements in their stable modifications at the reference temperature. For example, for the compound VC that means bcc V and graphite with the weighted sum ${}^{\circ}H_V^{bcc}(T_0) + {}^{\circ}H_C^{graphite}(T_0)$. Subtracting this sum from both sides of Equation (11) one obtain.

$$\begin{aligned} &{}^{\circ}G_m^{\phi}(T) - {}^{\circ}H_V^{bcc}(T_0) - {}^{\circ}H_C^{graphite}(T_0) \\ &= \Delta{}^{\circ}H_m^{\phi}(T_0) - T_0\,{}^{\circ}S_m^{\phi}(T_0) - \int_{T_0}^{T} {}^{\circ}S_m^{\phi}(T')dT' \end{aligned} \tag{12}$$

The term $\Delta{}^{\circ}H_m^{\phi}(T_0) = {}^{\circ}H_m^{\phi}(T_0) - {}^{\circ}H_V^{bcc}(T_0) - {}^{\circ}H_C^{graphite}(T_0)$ is the enthalpy of formation (per mole of formula units) of the metastabe ϕ phase referred to the enthalpy of the stable state of the elements at 298.15 K and 0.1 MPa. Equation (12) summarises the thermodynamic relations between the properties we focus on in the following, when constructing the ${}^{\circ}G_m(T)$ function for ϕ, namely the enthalpy of formation at $T_0 = 298.15K$ and the entropy at and above T_0.

Using different estimations based on experiments or first-principles calculations one can obtain the values of $\Delta^{\circ}H_m^{\phi}(T_0)$ and $^{\circ}S_m^{\phi}(T)$. Next one can insert these values in the right-hand side of the Equation (12) and integrate numerically to get values for the quantity $^{\circ}G_m^{\phi}(T) - ^{\circ}H_V^{bcc}(T_0) - ^{\circ}H_C^{graphite}(T_0)$. On the other hand, most phase diagrams calculations are performed by adopting a closed expression for the temperature dependence of the Gibbs energy. That is the reason why one assumed the Gibbs energy per mole of formula unit of the metastable ϕ phase due to the Equations (13) and (14),

$$^{\circ}G_m^{\phi}(T) - ^{\circ}H_V^{bcc}(T_0) - ^{\circ}H_C^{graphite}(T_0) = \Delta^{\circ}G_m^{\phi}(T) \tag{13}$$

and the temperature dependent function $\Delta^{\circ}G_m^{\phi}(T)$ was expressed as,

$$\Delta^{\circ}G_m^{\phi}(T) = a + bT + cT\ln T + dT^{-1} \tag{14}$$

Paper II, appended in this thesis, deals with modeling of ordered phases and just a brief explanation will be given here. Many intermetallic phases never disorder and as discussed above the compound energy formalism [34] can describe these phases successfully. However, some ordered phases can disorder. This behaviour is treated classical with the Bragg-Williams model [42]. In the Thermo-Calc software ordered phases are treated using the Bragg-Williams model [42], which turns out to be a special case of the compound energy formalism [34]. The ordered and disordered phases of the same type of structure are described with a single mathematical function containing configurational dependent, $G_m^{ord}(y)$, and configurational independent, $G_m^{dis}(x)$, parameters. The Gibbs energy for an ordered phase can be written as Equation (15),

$$G_m = G_m^{dis}(x_i) + \Delta G_m^{ord}(y_i^s) \tag{15}$$

where $G_m^{dis}(x_i)$ is the molar Gibbs energy of the disordered state, and $\Delta G_m^{ord}(y_i^s)$ the molar Gibbs energy for ordering. In the disordered state the ordering energy is zero but the ordered state always has a contribution from the disordered state. This is automatically provided in the model by expressing the ordering energy as Equation (16).

$$\Delta G_m^{ord}(y_i^s) = G_m^{ord}(y_i^s) - G_m^{ord}(y_i^s = x_i) \tag{16}$$

This treatment has been investigated in a paper by Kusoffsky et al. [43] and also by Dupin [44]. A four-sublattice model for the ordering was first used when treating fcc ordering in the binary Au-Cu system [45].

The method of extrapolating the thermodynamic properties of alloys into multicomponent systems is based on the summation of the excess energy of the lower-order sub-systems. Many different methods to perform this exist but the most widely used methods were developed by Kohler, Colinet, and Muggianu. More details about these methods can be found in different text books [18, 46]. The predominant method at the present time use the equation developed by Muggianu et al. [47] and that is also the method used in the Thermo-Calc software [16].

2.2 Kinetic Models

In a binary system, the flux of a species k obeys Fick's law as Equation (17),

$$J_k = -D_k \nabla c_k \tag{17}$$

where J_k is the flux of species k, D_k the diffusivity of k, and ∇c_k the concentration gradient of k. In a multicomponent system, the flux J_k will depend on the concentration gradients of all elements in the system. This condition is expressed by the Fick-Onsager law as Equation (18),

$$J_k = -\sum_{j=1}^{n-1} D_{kj}^{n} \nabla c_j \tag{18}$$

where n is the number of species and species n has been chosen as dependent. D_{kj}^{n} is the diffusion coefficient matrix and ∇c_j is the concentration gradient for species j. The diffusion coefficients form a matrix that is a product of two matrices, one kinetic containing mobilities and one thermodynamic containing second-order derivatives of the Gibbs energy. Andersson and Ågren [48] suggested that the atomic mobility should be modelled and stored in a kinetic database rather than the interdiffusion coefficients directly. The reason for that is that in an n-component system there are n mobilities and $(n-1)^2$ independent interdiffusion coefficients, and thus for systems with more than two components, there are fewer mobilities than diffusivities that need to be stored in the kinetic database.

Inspired by the CALPHAD method [17, 18] , Andersson and Ågren [48] suggested a similar method for treating kinetic data. They chose to represent the atomic mobility of the individual species in a multicomponent solution phase as a function of temperature, pressure and composition. From absolute-reaction rate theory arguments, they divided the mobility coefficient for element B in a given phase, M_B, into a frequency factor M_B° and an activation enthalpy Q_B, i.e.,

$$M_B = \frac{M_B^\circ}{RT} \exp\left(\frac{-Q_B}{RT}\right) \tag{19}$$

where R is the gas constant and T is the absolute temperature. The frequency factor M_B° is the product of the atomic jump distance and the jump frequency and has the units of m^2/s, Q_B has the units of J/mol. Both M_B° and Q_B will in general depend upon the composition, the temperature, and the pressure. Andersson and Ågren [48] described the composition dependency as a linear combination of the values at each endpoint of the composition space and a Redlich-Kister expansion [33].

The following describes the case Fe-Cr-V and only treat the fcc phase. The fcc phase is modelled with two different sublattices, one for the substitutional constituents (Cr, Fe, V) and one for the interstitials and vacant interstitial sites. For such a two-sublattice phase the following expression is used,

$$\mathbf{\Phi}_B = \sum_i \sum_j y_i y_j \mathbf{\Phi}_B^{i:j} + \sum_i \sum_{j \rangle i} \sum_l y_i y_j y_l \left(\sum_r {}^r\mathbf{\Phi}_B^{i,j:l} (y_i - y_j)^r \right) \tag{20}$$

where $\mathbf{\Phi}_B$ represents a composition dependent property, i.e. M_B° or Q_B. The upper right hand side indexes on the $\mathbf{\Phi}$'s indicate which species occupy the different sublattices, each separated by a colon. The commas separate different species interacting with each other on a certain sublattice. The different y terms are site fractions. The expression was later modified to make more reasonable interpolations.

Jönsson [49], utilising a work by Kucera and Million [50], suggested that one should expand the logarithm of the frequency factor M_B° rather than the factor itself. The frequency factor is thus given by,

$$M_B^\circ = \exp(\mathbf{\Phi}_B) \tag{21}$$

where $\mathbf{\Phi}_B$ is given by Equation (20). Thus the mobility M_B is expressed as Equation (22).

$$M_B = \exp\left(\frac{RT\mathbf{\Phi}_B}{RT}\right) \exp\left(\frac{-Q_B}{RT}\right) \frac{1}{RT} \tag{22}$$

For convenience, let us express the mobility as,

$$M_B = \exp\left(\frac{-\Delta G_B^*}{RT}\right)\frac{1}{RT} \tag{23}$$

where $\Delta G_B^* \equiv Q_B - RT\Phi_B$ is expanded by means of Equation (20), i.e. when calculating the mobility of Cr in the fcc phase for the Cr-Fe-V system one have the following expression,

$$\begin{aligned}
\Delta G_{Cr}^* &= y_{Cr} y_{Va} \Delta G_{Cr}^{*Cr:Va} + y_{Fe} y_{Va} \Delta G_{Cr}^{*Fe:Va} + y_V y_{Va} \Delta G_{Cr}^{*V:Va} \\
&+ y_{Cr} y_{Fe} y_{Va} \left[{}^0\Delta G_{Cr}^{*Cr,Fe:Va} + (y_{Cr} - y_{Fe})\, {}^1\Delta G_{Cr}^{*Cr,Fe:Va} \right] \\
&+ y_{Cr} y_V y_{Va} \left[{}^0\Delta G_{Cr}^{*Cr,V:Va} + (y_{Cr} - y_V)\, {}^1\Delta G_{Cr}^{*Cr,V:Va} \right] \\
&+ y_{Fe} y_V y_{Va} \left[{}^0\Delta G_{Cr}^{*Fe,V:Va} + (y_{Fe} - y_V)\, {}^1\Delta G_{Cr}^{*Fe,V:Va} \right]
\end{aligned} \tag{24}$$

where the $\Delta G_{Cr}^{*i:Va}$ and ${}^k\Delta G_{Cr}^{*i,j:Va}$ are expected to be linear functions of temperature.

The current approach to modelling the diffusion coefficients provides an efficient representation of the composition dependence in multicomponent systems. A relatively small number of parameters can represent a large quantity of diffusion data. From the mobility it is then possible to calculate various types of diffusivities. The tracer diffusion coefficient of an element B, D_B^*, can directly be calculated from Equation (25).

$$D_B^* = RTM_B \tag{25}$$

The chemical diffusivity is given by a more complex relation, where the concentration of one element n has been chosen as dependent of the others. The chemical or reduced diffusivity $\tilde{D}_{kj}^n$ can then be expressed as suggested by Andersson and Ågren [48],

$$\tilde{D}_{kj}^n = \sum_i (\delta_{ik} - x_k) x_i M_i \left(\frac{\partial \mu_i}{\partial x_j} - \frac{\partial \mu_i}{\partial x_n} \right) \tag{26}$$

where the Kronecker delta $\delta_{ik} = 1$ when $i = k$ and 0 otherwise and x_k is the mole fraction of element k. As the mole fraction of component k approaches 1, the chemical diffusivity $\tilde{D}_{kj}^n$ approaches the value of the tracer diffusivity of D_B^*.

2.3 Simulation of Coarsening and Diffusion

A precipitation process may often be regarded as divided into three different stages: nucleation, growth, and coarsening or Ostwald ripening. In the past, several authors have analysed precipitate coarsening [51, 52, 53, 54, 55] initially described by Ostwald [51]. The foremost theory was proposed independently by Lifshitz and Slyozov [54] and Wagner [55] and has become known as the Lifshitz-Slyozov-Wagner (LSW) theory. The coarsening process is described by a change in the mean particle size with the time of ageing. The mean particle size increases during coarsening with the net result that the number of particles decreases to maintain approximately the same volume fraction of the precipitate. The driving force for the coarsening process is the reduction in the free energy resulting from a decrease in the surface area per unit volume.

The coarsening model in the DICTRA software [56] uses the approximation that coarsening of a system can be described by performing calculations on a spherical particle of maximum size at the centre of a spherical cell. It is assumed that the particle size distribution obeys the Lifshitz-Slyozov-Wagner distribution [54, 55] , i.e., that the maximum particle size is 1.5 times the average size. In this model, a contribution from the interfacial energy is added to the Gibbs energy function for the particle according to Equation (27),

$$\Delta G_m = \frac{2\sigma V_m}{r} \tag{27}$$

where σ is the interfacial energy in J/m^2, r is the particle radius in meters, and V_m is the molar volume in m^3/mol. The simulation is based on local equilibrium [57] at the moving phase interface between the maximum size particles and the matrix, taking into account the contribution of the interfacial energy in Gibbs energy, see Figure 2. At the outer boundary of the calculational cell the composition is given by equilibrium with average size particles. The compositions of the matrix and carbide close to the phase interface can thus be evaluated from thermodynamic information and the interfacial energy. According to Equation (27) the particle of the maximum size will have a smaller Gibbs energy addition than the particles of average size, giving a difference in composition between the region close to the interface of the maximum particle and the matrix and the outer cell boundary. This difference will make the maximum particle grow. The particles maintain their spherical shape throughout the entire process. In order to maintain the total composition in the cell, the size of the cell will increase accordingly.

A flux, see Equation (18), of elements will pass the phase interface in both directions. The coarsening of the carbide means a movement of the phase interface. The rate of transformation will be controlled by the transport of the elements from and to the interface. Conservation of mass yields the following balance equation at the migrating interface between the matrix and the carbide,

$$v^{matrix} c_k^{matrix} - v^{carbide} c_k^{carbide} = J_k^{matrix} - J_k^{carbide} \quad (k = 1,...,n) \tag{28}$$

where v^{matrix} and $v^{carbide}$ are the interface migration rate seen from the matrix and from the carbide, respectively. c_k^{matrix} and $c_k^{carbide}$ are the concentrations in matrix and carbide close to the phase interface, and J_k^{matrix} and $J_k^{carbide}$ are the diffusional fluxes in matrix and carbide, respectively. The migrating rate is determined by solving the flux-balance equations. Three kinds of calculations are therefore required to solve the coarsening problem, equilibrium calculations, solving of diffusion equations, and solving of flux-balance equations. The DICTRA software [56] performs all these calculations numerically using two databases, one for thermodynamics and one for kinetics, see Figure 1. More detailed information about this coarsening model can be found in a work by Bjärbo and Hättestrand [58].

In the present work a new thermodynamic database, TOOL05, was used for the coarsening simulations. The development of the TOOL05 database is described in section 4. The kinetic database that was used was a modified version of the MOB database [59]. The Cr and V diffusion in pure fcc Fe was modified and is described in paper VI, all other kinetic information originates from the MOB database [59]. All the coarsening simulations in paper VI were also compared to simulations using the TCFE3 [31] and the MOB database [59].

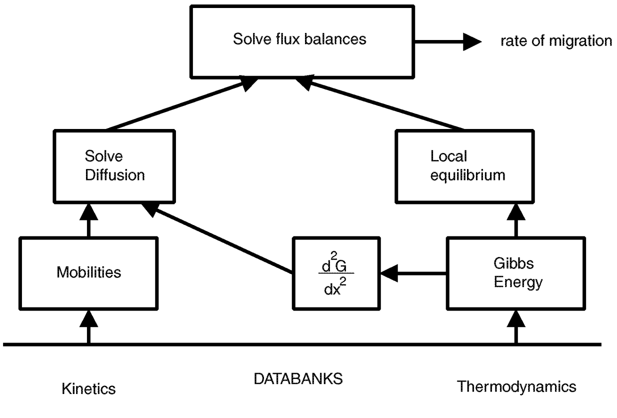

Figure 1. Schematic functions of the DICTRA software [56] for coarsening simulations.

The simulation is set up as a closed system with one spherical cell with an MC or M_7C_3 carbide at the centre surrounded by a matrix, see Figure 2. The initial conditions, which must be set for a simulation, are the radius r_1, the interfacial energy σ, the molar volume V_m, and the chemical composition of the phases and the size of the cell, r_2. Of course also the temperature and time must be given. In the present work the radius r_1 was measured experimentally and the size of the cell could be calculated from r_1 and knowledge of the fraction of the specific carbide, which was also measured in this work, see Equation (29).

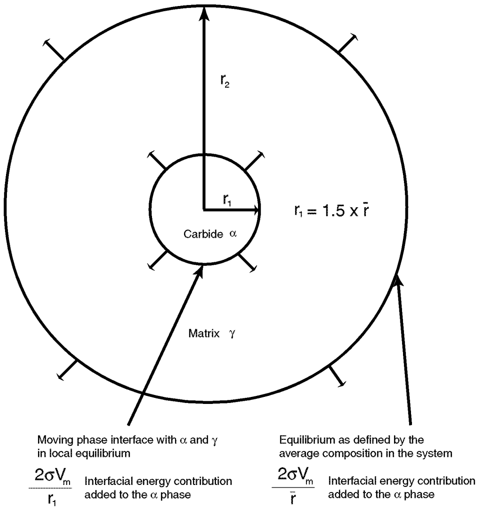
r_2
r_1
$r_1 = 1.5 \times \bar{r}$
Carbide α
Matrix γ
Moving phase interface with α and γ in local equilibrium
$\frac{2\sigma V_m}{r_1}$ Interfacial energy contribution added to the α phase
Equilibrium as defined by the average composition in the system
$\frac{2\sigma V_m}{\bar{r}}$ Interfacial energy contribution added to the α phase

Figure 2. The coarsening model in the DICTRA software [56]. A closed system with one spherical cell with a carbide at the centre surrounded by matrix.

$$v_f^{carbide} = \frac{V_{carbide}}{V_{cell}} = \frac{r_1^3}{r_2^3} \qquad \Rightarrow \qquad r_2 = \sqrt[3]{\frac{r_1^3}{v_f^{carbide}}} \tag{29}$$

where $v_f^{carbide}$ is the volume fraction of the carbide. The initial chemical composition of the phases and the molar volume V_m were calculated using Thermo-Calc [16] utilising the thermodynamic database TOOL05. The interfacial energy σ was evaluated from experimental information about coarsening in lower-order systems and these values were then used in the multicomponent system.

3. Experimental Techniques and Methodology

3.1 Model Alloys Design for Critical Phase Equilibria Experiments

To make a significant improvement of the thermodynamic description for tool steels and high-speed steels, new experimental phase equilibria information was needed. Within the present work a thermodynamic database, TOOL05, dedicated for tool steels and high-speed steels was developed. The previously available thermodynamic description, TCFE3 [31], was a valuable aid to calculate compositions of model alloys to be used for the experimental determinations. The idea was to produce model alloys, with as few elements as possible, that include the same combination of matrix and carbides that are found in commercial tool steels and high-speed steels. For the general validation, commercial alloy systems were included in the experimental program.

All the model alloys were designed and produced using pure elements. The designed compositions of the model alloys can be seen in different papers which are appended in this thesis, paper III, paper V, and paper VIII. Two of the model alloys have been designed and produced using powder metallurgy. The elements, total weight of 10 kg, were mixed and melted under argon atmosphere and subsequently gas atomisated using argon gas with a pressure of 50 bar. The powder was sized less than 250 μm and approximately 1 kg was put in a pure Fe capsule. A vacuum pump was used to lower the oxygen content inside the capsule, and pure N_2 gas at a pressure of 0.5 atm was then added. This procedure was repeated three times and finally the capsules were heat treated 1 hour at 1150 °C under a N_2 gas pressure of 0.5 atm. Directly after the powder had been nitrided and cooled down to room temperature inside the furnace, the capsule was closed and compacted by HIP at 1150 °C for 5 hours. This method was chosen to add nitrogen because these model alloys were designed to contain high amounts of nitrogen. It is not possible to produce these alloys using a conventional technique because the nitrogen will bubble out from the melt and result in an inhomogeneous structure.

The other model alloys produced within this thesis was produced by weighing in the respective elements to a total of 100 g and place the mixture in an aluminium oxide (Al_2O_3) crucible. The crucible was heated by induction in an electrical furnace under vacuum atmosphere until all the material melted. The alloys were then cast in a cold copper crucible into 100 mm long and 10 mm diameter bars.

3.2 Heat Treatments to Reach Phase Equilibria

Critical experiments have been performed in order to establish the equilibrium conditions in terms of phase fractions and compositions in the model alloys and the commercial alloys. Heat treatments were performed on the alloys at two different temperatures and holding times. The holding times to reach equilibrium states were based on a work by Coelho [60], who used two high-speed steel samples with equal overall composition but different starting microstructures. Coelho [60] heat treated both samples at 1250 °C and increased holding times until both the microstructures became similar. We assumed, based on the work by Coelho [60] and diffusion of substitutionally dissolved alloying elements, that equilibrium conditions are reached after 1000 hours at 1000 °C. By applying a reasonable activation energy, an equivalent time at a higher temperature can be estimated. In the present work the two selected heat treatments and holding times were 1000 hours at 1000 °C and 500 hours at 1150 °C.

The specimens produced from the commercial alloys had a length of approximately 50 mm with a cross section around 10x10 mm, whereas the specimens produced from the model alloys had a length of approximately 15 mm and a diameter around 10 mm. Before the specimens were placed in the furnace for heat treatment they were vacuum-sealed in quartz capsules to avoid oxidation and loss of elements due to evaporation. After the heat treatment the specimens were quenched in water and then cut into half the length and prepared by grinding and polishing for microstructure investigations.

Carbon diffuses interstitially and much faster than substitutionally dissolved atoms and therefore it is essential to avoid carburising or decarburising under the heat treatment. This was checked in the present work, through chemical analysis before and after the heat treatment. The analysis showed that no loss of C has occurred. It was also checked that impurities as Si, Mn, P, S, and O were within accepted limits in the model alloys.

3.3 Analysis of Heat Treated Samples

3.3.1 SEM Using Backscattered Electron Detector

All heat treated materials were subject to a SEM (Scanning Electron Microscope) backscattered electron analysis. The equipment used in the present work was a JSM-6400 scanning microscope. The different signals that can be detected originate from different volumes of the specimen, see Figure 3.

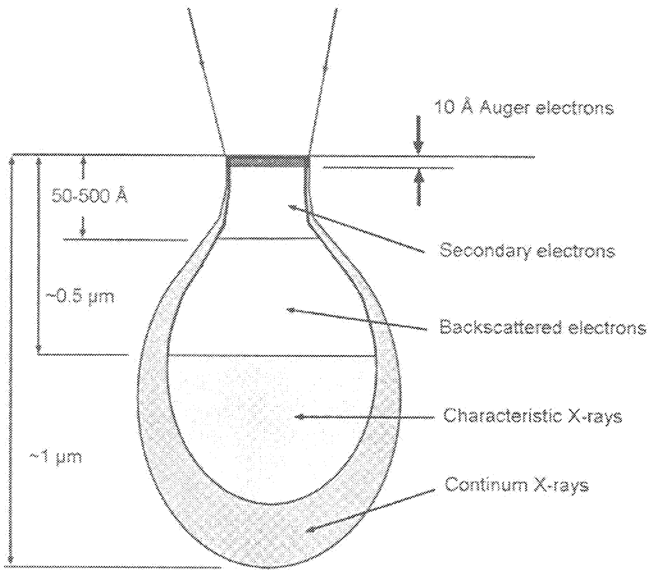

Figure 3. The Pear. Interaction volume between an electron beam and a bulk specimen. Different signals originate from different volumes in the specimen.

The yield of backscattered electrons is directly related to the atom number of the phase composition and gives therefore suitable discrimination of different phases. Heavy elements, for example molybdenum, will result in a brighter contrast in the micrograph. This phenomenon makes this method very adaptable to get good contrast for the different carbides, which one finds in tool steels and high-speed steels.

3.3.2 WDS/EDS Measurements with ASEM

To determine the composition of individual phases analysis was done using combined WDS (Wavelength Dispersive Spectrometer) and EDS (Energy Dispersive Spectrometer) measurements with ASEM (Analytical SEM). The connected software to handle the data for practical applications was the INCA system from Oxford Instruments.

Before one can use the X-rays emitted from the sample for analytical purposes one needs to know which of the many characteristic X-ray lines for each element is the most intense. This enables us to choose the best line to use as an index of how much of each element is present in the sample. Consequently the K_α line is most frequently used for analysis. However, it is not always possible to excite the K_α lines in an electron beam instrument since the energy required to knock out a K-shell electron becomes quite high for the heavy elements. One must look for other characteristic X-rays which are more easily excited in order to detect heavy elements (atoms with atomic number higher than 50). Fortunately the L_α lines have very suitable properties. The most efficient production of X-rays generally occurs when the bombarding electrons have about three times the X-ray energy. A study of Table 1 below will show that all elements in the alloys from the present work have at least one strong X-ray line with energy less than 8.5 keV and therefore there should be no difficulty in analysing all the elements, using the ASEM operating at 20-25 keV.

Table 1. The X-ray energy and associated wavelength of the K_α and L_α lines of the elements in the present work alloys. The respectively atomic number, Z, and atomic weight, A, is also shown.

Element	Atomic number	Atomic weight	K_α		L_α	
			E (keV)	Å (nm)	E (keV)	Å (nm)
C	6	12.011	0.2774	4.47	0	0
N	7	14.007	0.3924	3.16	0	0
Al	13	26.982	1.4866	0.83	0	0
Si	14	28.086	1.7398	0.71	0	0
V	23	50.942	4.9498	0.25	0.5113	2.42
Cr	24	52.996	5.4117	0.23	0.5729	2.16
Mn	25	54.938	5.8951	0.21	0.6374	1.94
Fe	26	55.847	6.3996	0.19	0.7048	1.76
Co	27	58.933	6.9254	0.18	0.7763	1.60
Mo	42	95.94	17.445	0.07	2.2932	0.54
W	74	183.85	59.311	0.02	8.3977	0.15

The EDS utilises a solid-state detector to analyse all X-ray photon energies simultaneously. The energy of each X-ray photon is characteristic of the element which produced it. The EDS microanalysis system collects the X-rays, sorts and plots them by energy, and automatically identifies and labels the elements responsible for the peaks in this energy distribution. The EDS data are typically compared with either known or computer-generated standards to produce a full quantitative analysis showing the sample composition.

As can be seen from Table 1 some elements have relatively similar values of the X-ray energies that will led to severely overlapped peaks in the EDS spectrum. To be able to measure the composition of these elements a combination of WDS and EDS is used to resolve overlapping peaks. For C, N, Al, Si, Mn, Co, Mo, and W analysis the WDS spectrometer was used in the present work. The principle of the WDS is that the X-rays coming from the specimen are filtered so that only X-rays of a chosen wavelength (usually the characteristic wavelength of the element of interest) are allowed to fall on a detector. The filtering is achieved by a crystal spectrometer that employs diffraction to separate the X-rays according to their wavelength. The resolving power of a crystal spectrometer is excellent and there is rarely a problem of adjacent lines overlapping. On the other hand, the disadvantages of a crystal spectrometer make its use very time-consuming and hence restricts its major applications to, e.g. detection of low concentrations, detection of light elements, and quantitative measurements of peak heights. In Table 2 the crystals for respectively element that were used in the present work is shown.

Table 2. The crystals for respectively element forWDS measurements.

Element	C	N	Al	Si	Mn	Co	Mo	W
Crystal	LSM80	LSM80	TAP	PET	LiF	LiF	PET	LiF

The crystal disperses X-rays by Bragg-reflection. The geometry of the WDS, illustrated below in Figure 4, is thus very important. All three components, the X-ray source (i.e. the sample), the crystal and the detector, must lie on the circumference of a circle known as the Rowland circle. To maximise the amount of surface area lying on the Rowland circle, the crystal is manufactured with a curvature on the side facing the X-ray source and the detector. As the angle formed by the three components changes by repositioning the crystal and the detector, X-rays of differing wavelengths are directed to the detector. In this way, a spectrum is produced.

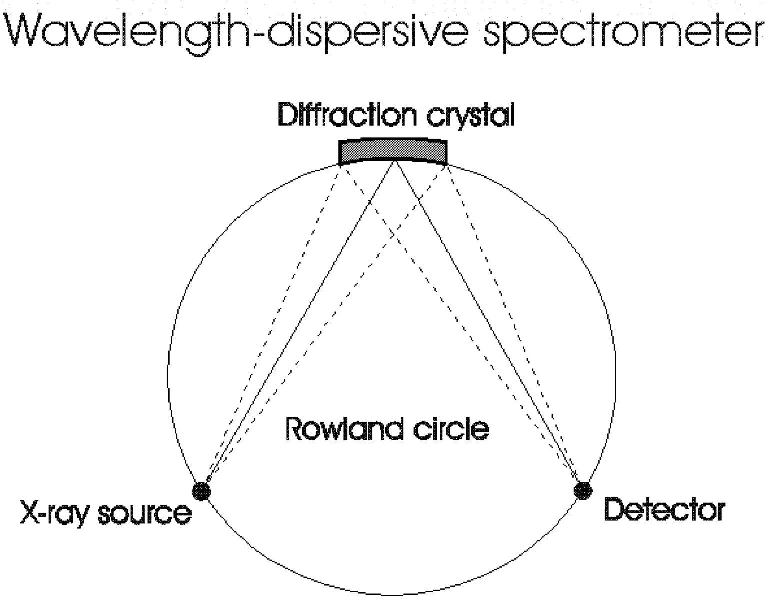

Figure 4. The Rowland circle.

One can summarise the use of EDS and WDS as follows. X-ray microanalysis in the scanning electron microscope is accomplished using EDS and/or WDS. EDS is more commonly applied due to its simplicity and speed, while WDS offers an important and often critical refinement of EDS data by providing;

- Analysis for light elements with at least an order of magnitude higher sensitivity than available (ultra thin X-ray window) EDS instruments.

- Resolution of several overlapped spectrum peaks for improved element specificity.

- Lowered detection limits over the entire periodic table.

- More accurate quantitative analyses.

An important work is to calibrate all the standards to fit the actually composition range before the measurements. In this case the carbon calibration was performed to be accurate around 10 mass percent carbon, to be able to measure the carbon content in the different carbides. The carbon content measured in the matrix will therefore be misleading, generally around 1 mass percent higher than expected. Also the N calibration was performed to be accurate around 10 mass percent nitrogen because this is approximately the amount nitrogen which dissolves in the MC carbide. All the other elements have reliable standards for measurements on the present alloys and in Table 3 below, all the standards used for respective element are shown.

Table 3. Standards used for respective element in the present investigation.

Element	**Standard used**	**Calibrated value**
C	Cr_7C_3	8.85 mass % C
N	Cr_2N	11.7 mass % N
Si	Pure	100 mass % Si
Mn	Pure	100 mass % Mn
Cr	Pure	100 mass % Cr
Mo	Pure	100 mass % Mo
V	Pure	100 mass % V
W	Pure	100 mass % W
Al	Al_2O_3	52.9 mass % Al
Co	Pure	100 mass % Co
Fe	Pure	100 mass % Fe

For each individual phase three to five measurements at different places in the specimen were done. This was judged sufficient since the size of the carbides after the long time heat treatments is relatively large. Problems can occur if the carbide size is too small (less than 4 µm) as influence of the surrounding elements can affect the measurements. The variation of the measured composition of a phase between different regions of the sample is small (+/- 3 %). The acceleration voltage was 20 kV and the beam current around 18 nA. The average value of the measurements for each element in each phase in the different alloys can be seen in the appended papers, papers I-V, paper VII and paper VIII.

3.3.3 Electron Microprobe Analysis

Electron microprobe analysis (EMPA) is a non-destructive method for determining the chemical composition of tiny amounts of solid materials. It was developed by R. Castaing in Paris as his 1950 Ph.D. dissertation. Commercial electron microprobes became available in the 1960s, and have become standard analytical tools.

EMPA uses a high-energy focused beam of electrons to generate X-rays characteristic of the elements within a sample from volumes as small as 3 µm across. The resulting X-rays are diffracted by analysing crystals (TAP, PET, LIF) and counted using gas-flow and sealed proportional detectors. Chemical composition is determined by comparing the intensity of X-rays from standards (known composition) with those from unknown materials and correcting for the effects of absorption and fluorescence in the sample. The electron microprobe is designed specifically for detecting and measuring characteristic X-rays. It uses an electron beam current from 10 to 200 nA, roughly 1000 times greater than that in a scanning-electron microscope (SEM). These higher beam currents produce more X-rays from the sample and improve both the detection limits and accuracy of the resulting analysis. Analysis locations are selected using a transmitted-light optical microscope, which allows positioning accurate to about 1 µm, a feature not available on an SEM. The resulting data yield quantitative chemical information in a textural context. Variations in chemical composition within a material, such as a mineral grain or metal, can be readily determined. The electron microprobe can quantitatively analyse elements from fluorine (Z=9) to uranium (Z=92) at routine levels as low as 100 ppm.

In this work a SEMQ-ARL electron microprobe equipment was used to measure the C, N, and V content in the matrix phase in some of the specimens.

3.3.4 EBSP Analysis

The electron back scattering patterns (EBSP) technique is based on the discovery [61] and application [62] of Kikuchi patterns. Remarkable progress [63, 64, 65] in the use of this technique has been made in the past 20 years. The stationary beam is focused to a fine point on a highly tilted sample and the diffracted back scattered electrons form Kikuchi patterns on a phosphor screen. The orientation of the local lattice can be obtained by digitising two appropriate zones in the Kikuchi pattern. In fcc material, two zones on the band passing through <111>, <112>, <114> and <332> are usually selected for digitising. Furthermore, the orientation information of an interesting area can be collected by an electron beam movement controlled by a computer with selected step size.

In this study, EBSP work was carried out using a Field Emission Gun SEM (FEG-SEM) LEO 1530 with GEMINI column interfaced to a workstation with orientation image microscopy software. The sample was mounted on a pre-tilted sample holder with tilt angle of 70° for better pattern quality. The geometry of the sample setup is shown in Figure 5. The acceleration voltage and working distance were maintained at 20 kV and 20 mm, respectively. This technique was used to determine unknown phases in some samples.

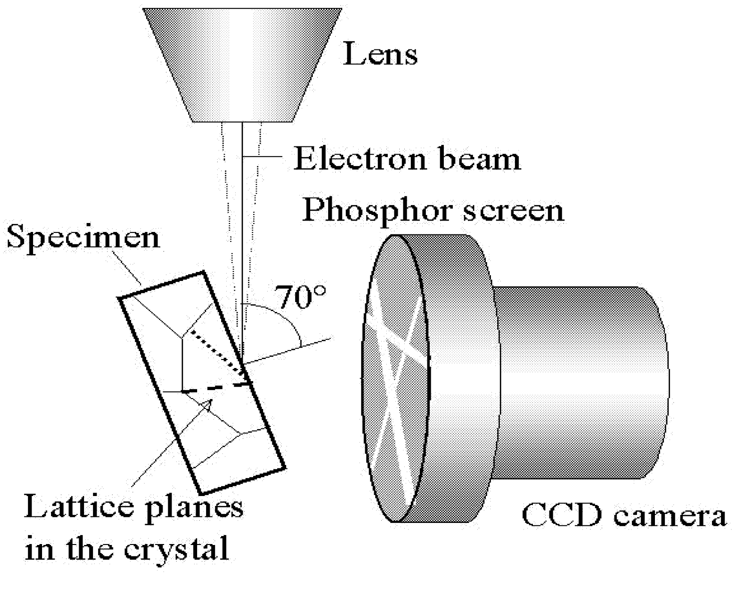

Figure 5. The geometry of the sample setup for the EBSP measurements.

3.3.5 MicroGOP Analysis

The MicroGOP 2000/S software [66] was used to measure the phase fractions and the carbide size distribution from SEM micrographs. This software is a complete application for image processing and quantitative image analysis. It is based on a very sensitive separation system of different grey scales. All the analysis of phase fractions was based on ten micrographs with 1000 times magnification taken from different places of the specimen to get good reliability on the values. For the commercial alloys manufactured by conventional technique fifteen micrographs with 1000 times magnification and also some with lower magnifications were taken due to the irregularity in the carbide distribution.

The carbide size distribution was measured on some alloys. These alloys have been manufactured by powder metallurgy and the measurements are based on 10 randomly taken micrographs with 1000 times magnification. Two different types of values of the carbide diameter are given for the above analysis. The first is Dmax (maximum diameter) which reproduces the maximum width of the carbide in the micrograph and the second one is EqD (equal diameter) which reproduces the diameter if the total area fraction is assumed to be a circle.

3.4 Experimental Results and Discussion

Heat treatment experiments at 1000 °C and 1150 °C have been performed on various model alloys and commercial alloys manufactured with different methods as conventional, powder metallurgy and spray forming. After the heat treatments the specimens were analysed by means of, SEM, EDS/WDS, EBSP, EMPA, and MicroGOP. This experimental work has lead to a large amount of new information on important aspects of tool steels and high-speed steels.

All the new experimental information in both model alloys and commercial alloys are presented in the appended papers in this thesis. During this PhD work 21 commercial alloys have been included in a large experimental investigation, which is presented in paper XI. This report is confidential until year 2015 but many results of the commercial alloys from this investigation are presented in the papers appended in this thesis. The experimental results from the model alloys are presented in the appended papers. Therefore, only concluding results will be discussed in this section.

First of all, one must emphasise that it is very important to ensure that equilibrium is reached in this kind of experiments. The comparison of the microstructure of the initial state of the model alloys and the heat treated state shows that the carbides that occur in the initial state have been partly dissolved and reprecipitated at the heat treatment temperatures. The microstructure of the commercial alloys has coarsened with 3 to 10 times compared to the as-received condition, see Figure 6. In Figure 7 the microstructure evolution during heat treatment is shown for two different model alloys. The phase compositions were measured in the largest carbides found in the different samples. In most of the cases the mean carbide diameter is 5-10 μm, which is enough to be able to perform accurate measurements. The measured compositions in both model alloys and commercial alloys should thus reflect the equilibrium state at the different heat treatment temperatures. Figure 8 shows an output from an EDS/WDS measurement. An indication that the measurement has satisfactory accuracy is that the total amount of analysed elements is as close to 100 as possible. Since the equipment that was used was calibrated to be able to perform accurate measurements on the carbides containing high amounts of different elements, the measurements of elements in small amounts in the matrix were less satisfactory. In particular, this was the case for the content of C, N, and V in the matrix phase. To account for these deviation electron microprobe analyses were performed of these elements in some samples to determine the different solubility limits.

A second important conclusion of the present work is that the measured values of the composition in the different phases all show large deviation from values calculated using the old thermodynamic description. This is especially true for the distribution of the carbide-forming elements inside the carbides. Also the measured phase fractions were poorly predicted using the old thermodynamic description, i.e. the prediction of individual phase stabilities was not satisfactory. Regarding the M_6C carbide it was found that it dissolves significant amounts of Si. This effect was not included in the thermodynamic model previously. Also a large amount of Co was discovered to dissolve in the M_6C carbide.

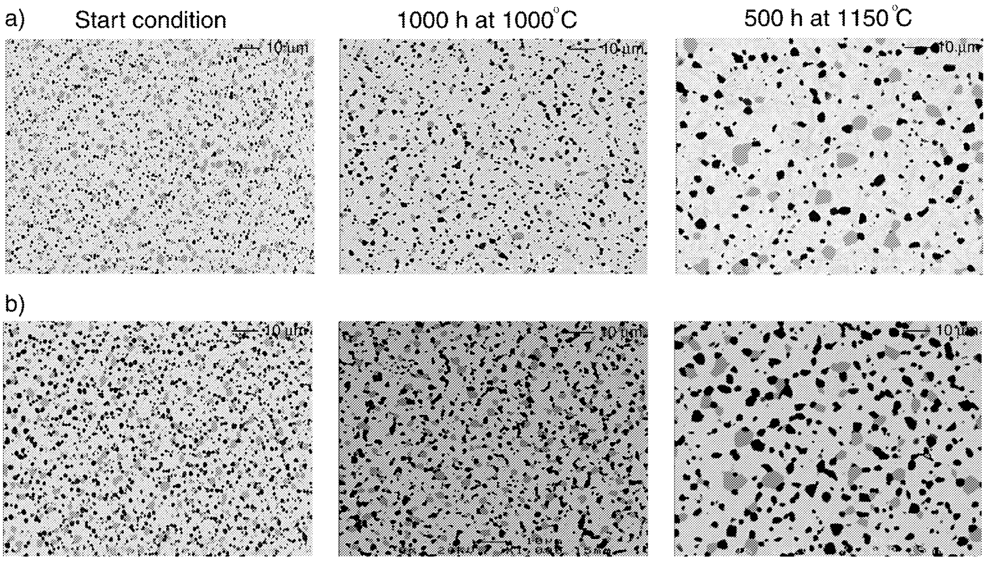
a)
Start condition
1000 h at 1000°C
500 h at 1150°C
b)
10 µm

Figure 6. Microstructure evolution from the start condition to the heat treated structures of two different commercial alloys a) and b). Black carbides are MC and grey are M_7C_3.

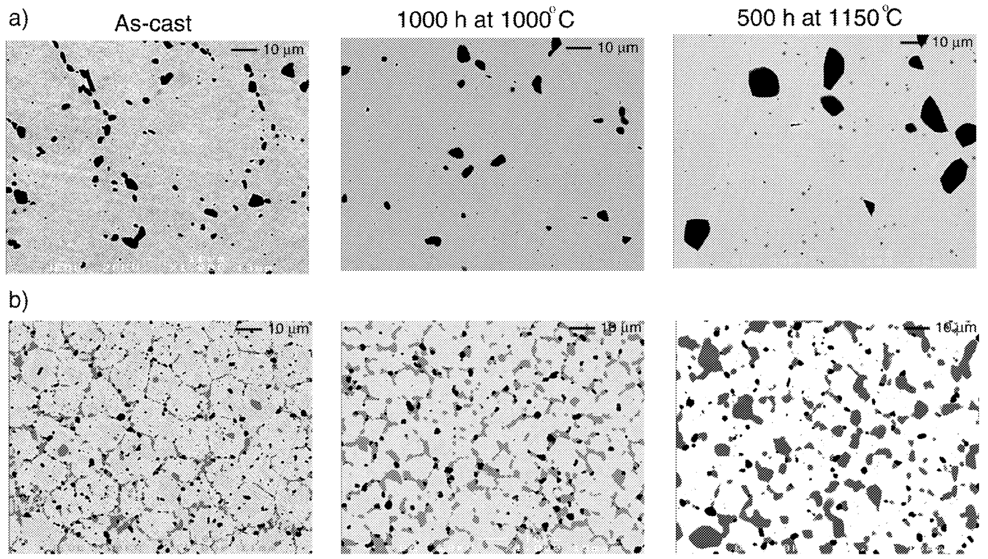
a)
As-cast
1000 h at 1000°C
500 h at 1150°C
b)
10 µm

Figure 7. Microstructure evolution from the start condition to the heat treated structures of two different model alloys a) and b). Black carbides are MC and grey are M_7C_3.

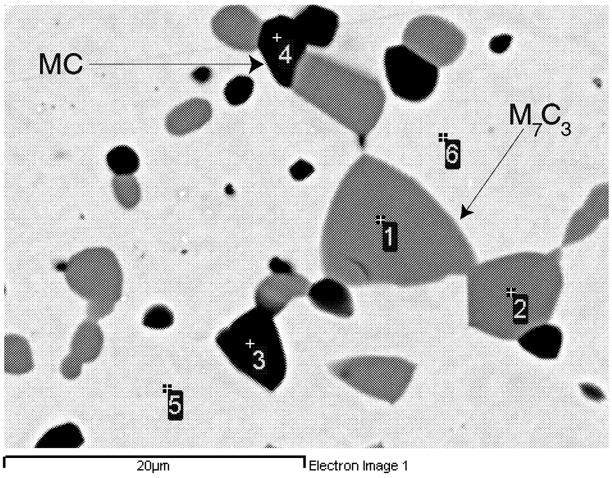

Spectrum	C	V	Cr	Fe	Mo	Total
1	9.11	17.95	42.01	27.49	3.71	100.27
2	9.20	17.97	42.03	27.40	3.46	100.06
3	15.74	64.06	8.31	3.23	8.78	100.13
4	16.04	63.02	8.85	4.46	8.58	100.96
5	0.76	2.07	10.77	84.94	1.94	100.48
6	0.78	2.08	10.92	84.89	1.70	100.37

All results in Weight Percent

Figure 8. EDS/WDS measurement showing the composition of different phases for a model alloy heat treated at 1150 °C for 500 h.

4. Development of a New Thermodynamic Database Utilising the new Phase Equilibria Information

4.1 Work Plan

In the beginning of this work the available thermodynamic descriptions were used as input for merging a starting version of the new thermodynamic database. Next, errors and discrepancies between calculated values and the new experimental information on the commercial alloys were identified. From this information model alloys were selected for critical experiments on the phase equilibria. Also available experimental information in the important lower-order systems was collected from the literature. The procedure of selecting experimental data, choosing the model and performing an adjustment to the experimental data is called assessment or evaluation. It is a task that requires great skill since the experimental information many times is contradictory and choices have to be made on which sources to trust. The new experimental investigation performed in this work was necessary due to lack of important information on the carbide systems in tool steels and high-speed steels. After every new evaluation or modification of a lower-order system the result was verified against the phase equilibria information in commercial multicomponent alloys. This procedure was repeated many times and in each cycle a new lower-order system was improved leading to a total improvement of the thermodynamic description for the multicomponent systems. This kind of work is schematically shown in Figure 9 below.

Some of the lower-order systems are the same as used in other thermodynamic databases e.g. the one for cemented carbides, developed first within the CAMPADA project [67] and then further developed within the Centre of Computational Thermodynamics (CCT) [68]. Therefore at the final step that thermodynamic database was partially merged with the new tool steel database. All this work has led to present TOOL05 database. The different versions of the TOOL databases stand for the year when it was released.

In the Figure 9 one can see which systems have been evaluated and modified within this work. Most of the systems are binary and ternary systems but also some quaternary systems have been evaluated. Carbides containing more than two sublattices may require assessment of quaternary systems. This is the case for the M_6C carbide which contains four sublattices. One usually does not consider higher-order systems than quaternaries.

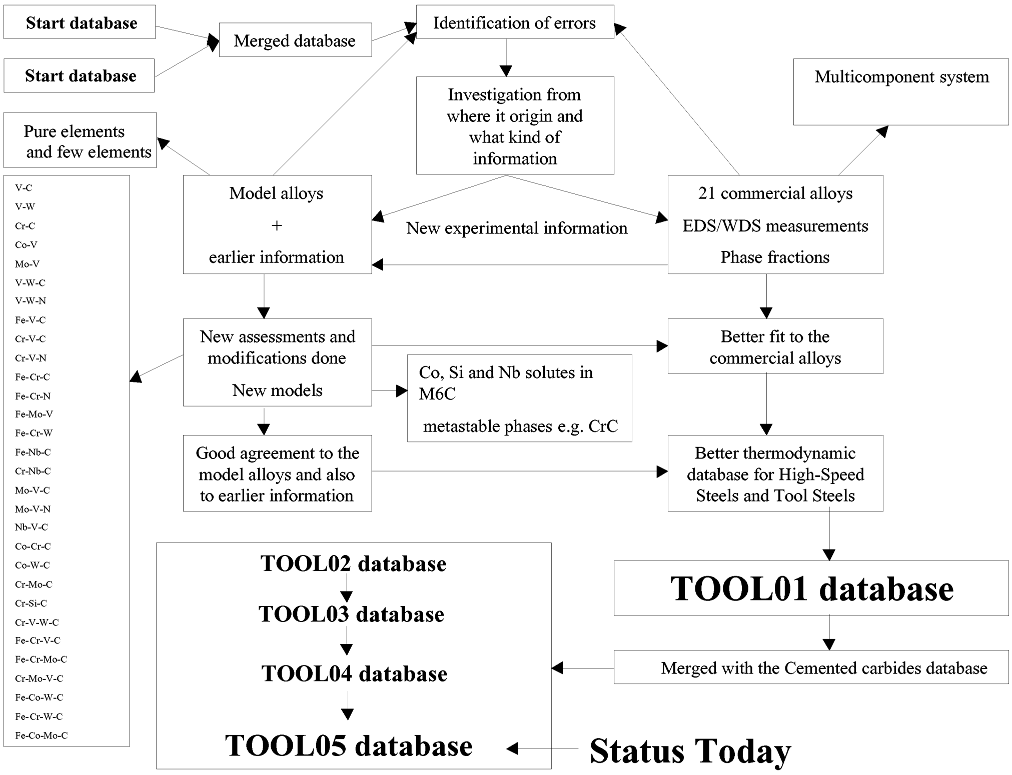
Start database
Start database
Merged database
Identification of errors
Investigation from where it origin and what kind of information
Multicomponent system
Pure elements and few elements
V-C
V-W
Cr-C
Co-V
Mo-V
V-W-C
V-W-N
Fe-V-C
Cr-V-C
Cr-V-N
Fe-Cr-C
Fe-Cr-N
Fe-Mo-V
Fe-Cr-W
Fe-Nb-C
Cr-Nb-C
Mo-V-C
Mo-V-N
Nb-V-C
Co-Cr-C
Co-W-C
Cr-Mo-C
Cr-Si-C
Cr-V-W-C
Fe-Cr-V-C
Fe-Cr-Mo-C
Cr-Mo-V-C
Fe-Co-W-C
Fe-Cr-W-C
Fe-Co-Mo-C
Model alloys + earlier information
New experimental information
21 commercial alloys
EDS/WDS measurements
Phase fractions
New assessments and modifications done
New models
Co, Si and Nb solutes in M6C
metastable phases e.g. CrC
Better fit to the commercial alloys
Good agreement to the model alloys and also to earlier information
Better thermodynamic database for High-Speed Steels and Tool Steels
TOOL01 database
Merged with the Cemented carbides database
TOOL02 database
TOOL03 database
TOOL04 database
TOOL05 database
Status Today

Figure 9. Outline of the development of the new thermodynamic database.

4.2 Verification of Results Using Commercial Tool Steel Alloys

An attractive feature of the experimental data that have been evaluated as described in section 4.1 is that it is possible to combine all the thermodynamic data describing different binary and ternary systems and make calculations for multicomponent alloys. The predictive potential of the CALPHAD method [17, 18] will be demonstrated in this section demonstrating that the different thermodynamic descriptions of lower-order systems can be combined to yield an accurate description of higher-order systems. To verify the improvements made in the present work 21 commercial alloys were considered. For all these alloys phase equilibria information about the composition in the individual phases as well as their fraction have been experimentally determined.

In Table 4 it is summarised how the commercial alloys have been manufactured and the total amount of carbides at the austenitising temperature is shown. In addition the type of carbides is indicated. More detailed experimental information about the commercial alloys can be found in the appended papers.

Table 4. Manufacturing technique of the commercial alloys, total amounts of carbides and type of carbide.

Commercial Alloy	Manufacturing Technique	Total amount of carbides in % at the austenitising temperature	MC	M_7C_3	M_6C
1	Conventional	2.60		X	
2	Conventional	3.40		X	
3	Conventional	15.9		X	
4	Spray Forming	12.8	X		
5	Spray Forming	10.2	X		
6	Spray Forming	21.0	X	X	
7	Spray Forming	25.2	X	X	
8	Powder Metallurgy	25.5	X		X
9	Powder Metallurgy	14.4	X	X	
10	Powder Metallurgy	17.2	X	X	
11	Powder Metallurgy	25.8	X	X	
12	Powder Metallurgy	14.9	X		X
13	Powder Metallurgy	15.8	X		X
14	Powder Metallurgy	22.0	X	X	
15	Conventional	14.5	X	X	
16	Conventional	11.4	X	X	
17	Powder Metallurgy	22.8	X	X	
18	Powder Metallurgy	17.8	X		X
19	Powder Metallurgy	23.9	X		X
20	Powder Metallurgy	15.4	X		
21	Powder Metallurgy	24.0	X	X	

Thermodynamic calculations have been performed using the old thermodynamic database and the new one developed in this work. Comparison with all the experimental information on commercial alloys has been made and the rate of improvement can be described as follows.

- Accuracy in predicting the correct phase.

Before	**84 %**
Now	**97 %**

- Accuracy in predicting the correct phase fractions.

Before	**20-30 % error**
Now	**< 10 % error**

- Accuracy in predicting the correct phase composition.

Before	**35-40 % error**
Now	**< 10 % error**

As can be seen, the new thermodynamic description much superior to the old one. All the commercial alloys contain different amounts of different alloying elements and have also been manufactured in different ways, which indicates the wide range of possibilities using this new thermodynamic database. This is very important information to the tool steel making companies. Of course all the lower-order systems, which have been evaluated and modified, have been improved as well. This is described in detail in the appended papers.

4.3 Status Today and Possible Applications

The new thermodynamic database dedicated for tool steels and high-speed steels allows calculations of several different thermodynamic properties in multicomponent systems with high accuracy. This section demonstrates some important applications in design and development of new alloys.

Through thermodynamic calculations one can easily and rapidly calculate the phase equilibria of a commercial multicomponent alloy. Figure 10 shows a thermodynamic calculation of the fractions of different phases as function of temperature for a given alloy composition. This information can be used to optimise the amount of different carbides which will influence the mechanical properties. This information is also very valuable when optimising the heat treatment temperatures. For the alloy shown in Figure 10 one wants to avoid the formation of the brittle $M_{23}C_6$ carbide during austenitising and the subsequent cooling. As can be seen, $M_{23}C_6$ will start form below 950 °C.

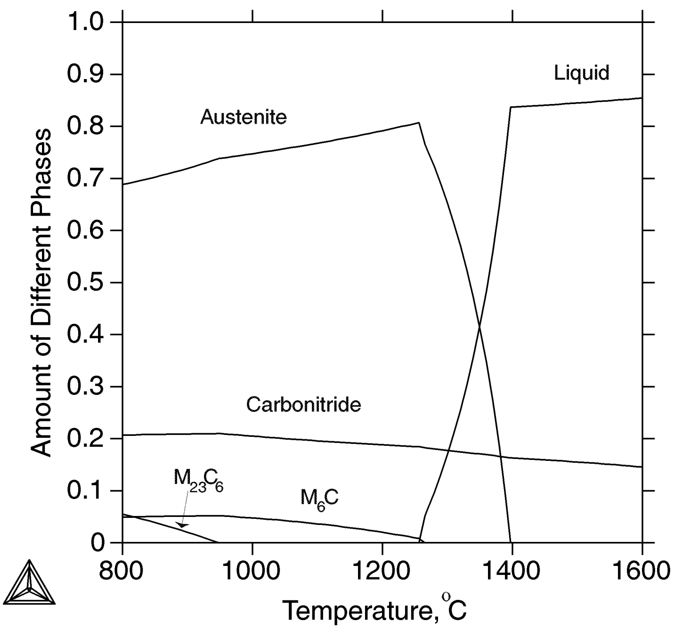

Figure 10. Calculated diagram using the new thermodynamic database for a given alloy composition showing how the different amount of phases vary with the temperature.

During the alloy design and development it is also important to know the different solubilities of different elements in different phases. The composition of the matrix phase at the austenitising temperature will directly influence the secondary carbide precipitation during the tempering process. That precipitation partly controls the mechanical properties of the alloy.

Another important phenomenon is how nitrogen substitutes carbon going from MC carbide to carbonitrides. This has not been satisfactory predicted by older databases. In Figure 11 it is shown, for a commercial alloy with a given composition at 1150 °C, how the increasing amount of nitrogen changes the distribution of other elements in the carbonitride significantly. This will also, of course, influence on the stability of the other stable phases and the composition of those phases.

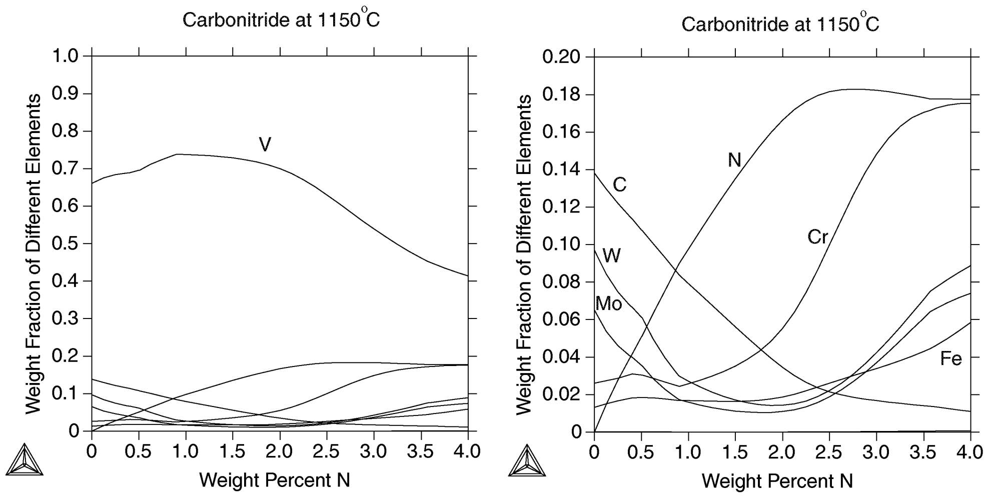

Figure 11. Diagrams calculated with the new thermodynamic database showing how the increasing amount of nitrogen changes the composition of the carbonitride at 1150 °C for an alloy with a given composition.

One can clearly see in Figure 11 that increasing amounts of nitrogen leads to a strong decrease in carbon content. Moreover, the amounts of tungsten and molybdenum decrease, whereas the chromium content increases very much when the nitrogen content reaches 2 mass %. The vanadium content starts to decrease when the nitrogen content reaches 2 mass %, even though the content increases at lower nitrogen contents. This effect is unexpected since vanadium has a larger affinity to nitrogen than chromium. This phenomenon will of course influence the properties of the specific phase under consideration. It is therefore important to be able to predict such effects through thermodynamic calculations.

A reliable thermodynamic description of nitrogen in these alloy systems allows thermodynamic calculations of the effect of external nitrogen gas pressure during solidification. This is done using the approximation of Siwert's law as described in Equation (30).

$$P_{N_2} = a_N^2 \tag{30}$$

In Figure 12 it is shown how these kinds of calculations can be visualised using different types of nitrogen pressures during the solidification process for a commercial alloy. One can clearly see when the alloy passes the ferrite state during the solidification where the nitrogen solubility is very low around 1410 °C. After that the solubility increases again and gets higher towards lower temperatures. Especially when the carbonitride phase forms which can dissolve large amounts of nitrogen. In this case the partial nitrogen gas pressure is the same as the total pressure even though the total pressure was put to 1 atm in the calculations, consistently. This is a reasonable approximation because 100 bar is a too low pressure to influence the transformation between e.g. ferrite and austenite.

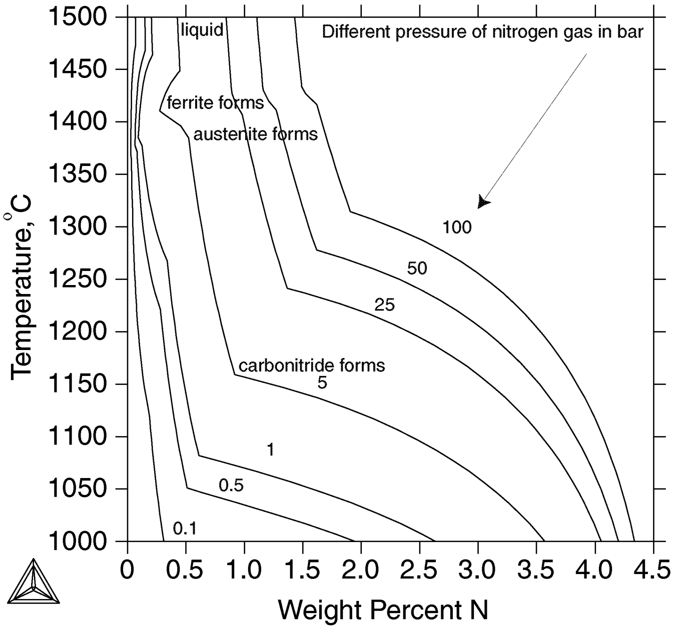

Figure 12. Calculated effect of external nitrogen pressure on the total solubility of nitrogen in the alloy during solidification.

To summarise the status of the new developed thermodynamic database accurate predictions of various thermodynamic properties can be done within the temperature range between 950 °C up to 1200 °C. The ingoing composition range of different commercial alloys within these predications can be made with high accuracy is shown in Table 5 below.

Table 5. Composition range where the new thermodynamic database gives reliable results.

Alloying Element	Composition range in mass %
C	0-3
N	0-3
Si	0-1.5
Mn	0-1.5
Cr	0-20
Mo	0-10
V	0-15
W	0-15
Ni	0-3
Co	0-15

The new thermodynamic database can also be applied for different kind of diffusion simulations utilising the DICTRA software [56]. Diffusion simulations of solidification intervals for different steel grades can be performed through coupling kinetic descriptions with the new thermodynamic database. It is then possible to predict the micro segregation behaviour. Such simulations based on experimental measurements of the dendrite arm distance may be applied to predict the time needed to level out the micro segregation or dissolve the carbides which have formed from the last solidified liquid. This kind of diffusion simulations have been done in a work by Bruce et al. [69], and the simulation results have also been verified experimentally in that work.

As described in chapter 5 the new thermodynamic database has made it possible to also predict carbide coarsening. For these kinds of simulations an accurate kinetic description is necessary. Therefore a new kinetic description has been developed in this thesis, as described in paper VI and in the next chapter. Figure 13 shows a carbide coarsening simulation performed within this work and a comparison with new experimental data for a commercial tool steel. One can clearly see that the M_7C_3 carbide coarsens much faster than the MC carbide.

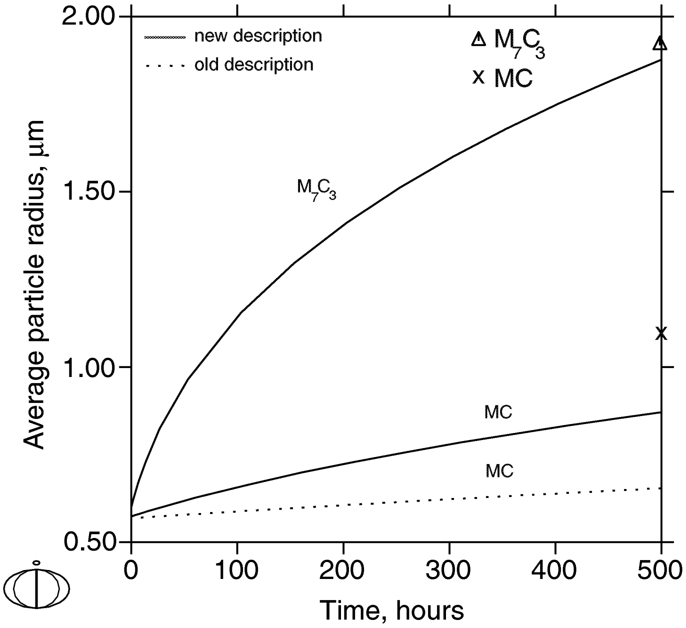

Figure 13. Calculated carbide coarsening at 1150 °C for a commercial tool steel compared to experimental values using both the old and the new thermodynamic descriptions. Note that the M_7C_3 carbide was not predicted to be stable using the previous thermodynamic description.

In the microstructure shown in Figure 14 one can clearly see a light grey phase which is $M_{23}C_6$ carbide. This brittle $M_{23}C_6$ carbide must be dissolved through a heat treatment due to its negative effect on the mechanical properties. Figure 15 below shows a simulation of dissolution of the $M_{23}C_6$ carbide surrounded by an fcc matrix at two different temperatures, using the new thermodynamic and kinetic descriptions and the old descriptions. If the temperature 1150 °C is used one must heat treat 15-16 hours to dissolve the carbides. An increased temperature to 1200 °C will decrease the heat treatment time to 2-3 hours.

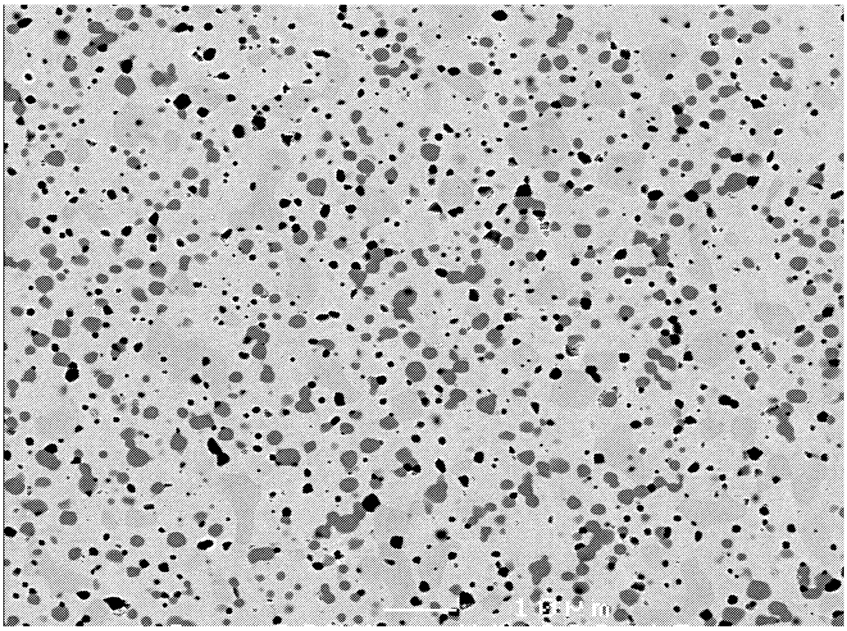

Figure 14. Microstructure of a commercial alloy after heat treatment in 1000 hours at 1000 °C. Black carbides are MC, grey carbides are M_7C_3 and light grey carbides are $M_{23}C_6$.

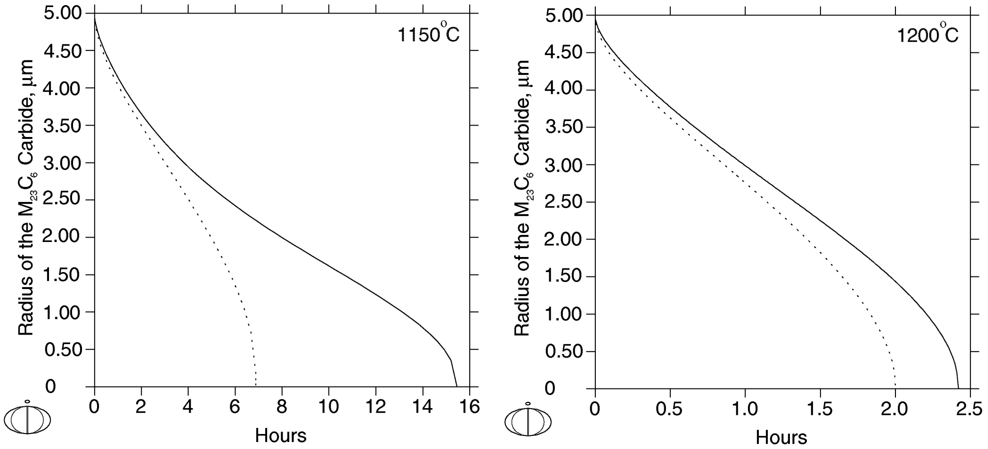

Figure 15. Dissolution simulations of $M_{23}C_6$ carbide in a commercial alloy at two different temperatures. The new thermodynamic and kinetic descriptions was used for the unbroken lines and the previous descriptions was used for the dotted lines.

The predicted time for complete dissolution of the $M_{23}C_6$ carbide is much faster using the old descriptions as shown in Figure 15, especially at the lower temperature. The main reason for this is that the new thermodynamic description describes the stability of the $M_{23}C_6$ carbide much better than the old. In this work it has been experimentally determined that the fraction of the $M_{23}C_6$ carbide at 1000 °C is 9.7 %. This phase was not predicted to exist at all with the old thermodynamic description whereas the new one predicts 9.5 %, see Figure 16. This improvement affects the diffusion simulations of $M_{23}C_6$ carbide dissolution and the new predictions should be much more reliable.

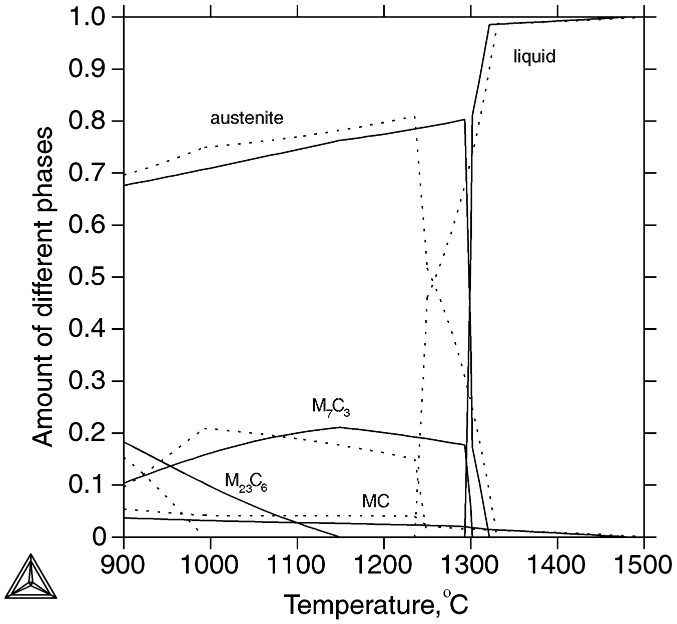

Figure 16. The phase fractions as function of temperature for the commercial alloy above using the new TOOL05 database (unbroken line) and the old TCFE3 database (dotted line).

5. Coarsening Experiments and Simulations to Assess Tracer Diffusion Data

5.1 *Assessment of Tracer Diffusion Data for Mobility Evaluation Using New Experimental Coarsening Information*

This work concerns only the coarsening process and does not deal with nucleation and growth. The initial state, i.e. phase fractions and composition, are then close to equilibrium. The coarsening simulations together with new experimental information at 1000 °C and 1150 °C were used to assess available tracer diffusion data for Cr and V in pure fcc Fe, as described in more detail in paper VI. After choosing the data, which was most consistent with the coarsening information, the mobilities were evaluated and finally the interfacial energy could be fitted against experimental information. The model is not a fully predictive model which begins with a single supersaturated matrix phase as described in the referred papers in paper VI. All input data, except the carbide size, such as phase fractions and compositions, can be found through equilibrium calculations, using the new thermodynamic database. The carbide initial size is relatively easy to measure and is not critical for the simulation results.

The main result of this work is that the mobilities of Cr and V in pure fcc Fe were changed to fit the new coarsening experiments. The new experimental information made it possible to chose which tracer diffusion data to trust. After the mobilities were evaluated the interfacial energy was adjusted to the new coarsening experiments and available ternary information. This was kept constant when applied in multicomponent systems yielding satisfactory results.

5.2 *The Influence of the Thermodynamic Description*

For the coarsening simulations in this work, in alloys with high content of Cr and V, the new thermodynamic description has played an important role. The new description of the distribution of Cr and V in the carbides under consideration has been improved significantly. This information is used as input data for the diffusion simulations. More important are the improved phase stabilities between different carbides, which are used in the coarsening model to describe the mass balance in the system. For two commercial alloys isopleths were calculated with the new thermodynamic description, showing that both alloys are predicted to lie inside the three phase area, fcc, MC, and M_7C_3 phase, in the temperature range for the coarsening experiments, see Figures 17 a and b (left). Figures 17 a and b (right) show how the stability of different phases vary with temperature for each commercial alloy, respectively, using the old and the new thermodynamic description. The M_7C_3 carbide is now much more stable at higher temperatures and the phase fraction is also larger than before, all this supported by recent experimental information presented in paper III. Since the previous thermodynamic description did not predict the M_7C_3 carbide to be stable at 1150 °C, for both of the commercial alloys shown in Figures 17 a and b (right), it is impossible to perform diffusion simulations of M_7C_3 carbide coarsening using that description.

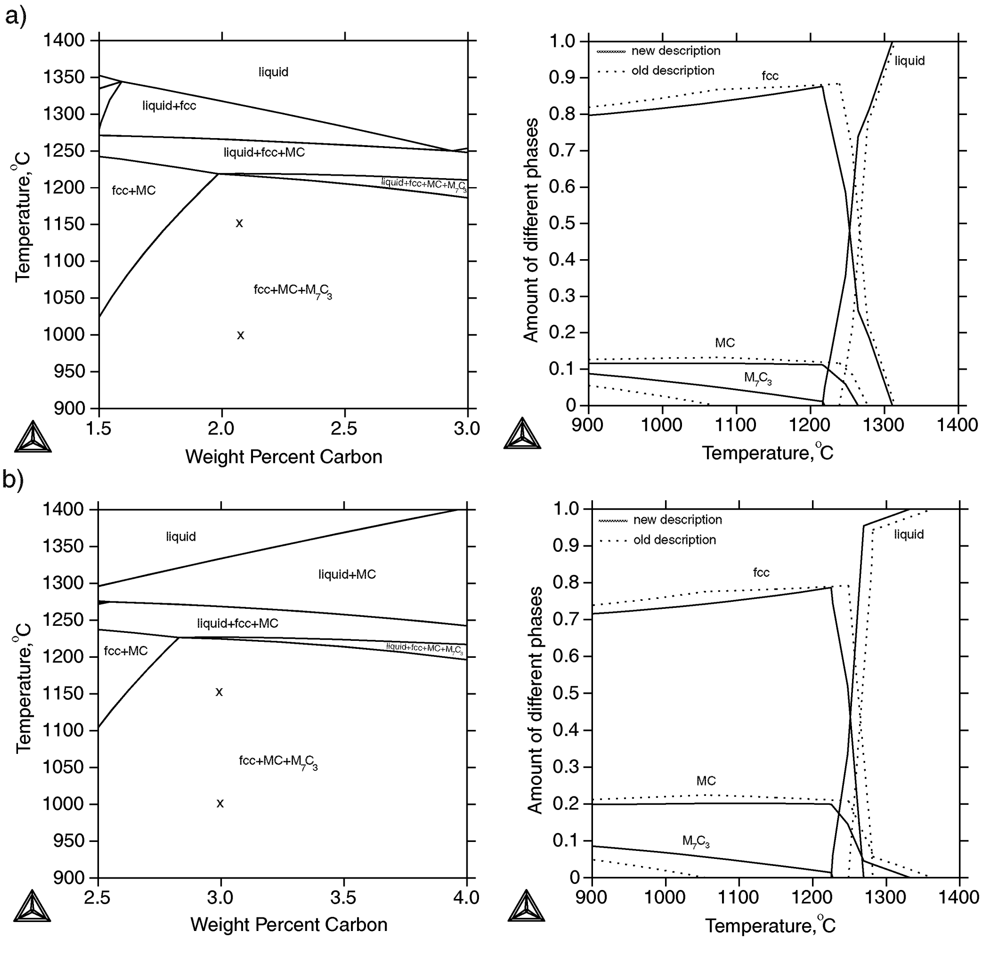

Figure 17. Calculated isopleths and diagrams showing how the different phase fractions vary with temperature at a given composition for the two commercial tool steels 1 (a) and 2 (b).

5.3 The Influence of the Interfacial Energy

Another important quantity for the coarsening rate of the carbides is the interfacial energy. The precipitation and growth process in alloys has a large contribution to the driving force from the supersaturated matrix phase. In the case of coarsening this is not the case. During the coarsening process the reduction in total interfacial energy is the driving force for the process.

The interfacial energy is very difficult and perhaps impossible to determined experimentally in multicomponent systems. Turnbull et al. [70] have suggested a combined theoretical and experimental method for determining the interfacial energy between crystal nuclei and the corresponding liquids but it can only be applied to binary systems and with large uncertainty. Therefore it was decided in the present work to determine the interfacial energies for the MC and M_7C_3 carbides using ternary coarsening experimental information using both the new thermodynamic description and the new kinetic description developed within this work. The interfacial energy was thus treated as an adjustable parameter to fit the experimental coarsening data. It was chosen here to adjust the interfacial energy of the MC and M_7C_3 carbides to be able to represent the experimental values from Wey et al. [71]. Also the new experimental coarsening information produced in the present work was taken under consideration as explained in paper VI. It was found that the interfacial energy of the M_7C_3 carbide is almost twice as large as that of the MC carbide.

6. Summary of Appended Papers

6.1 Paper I

A Thermodynamic Analysis of the Mo-V and Mo-V-C Systems

In this paper a new thermodynamic evaluation of the binary Mo-V system and the ternary Mo-V-C system, using the compound energy formalism [34] for the Gibbs energy of individual phases, is presented. The binary Mo-V system is characterised by complete solid solution of bcc structure and the phase diagram is rather simple with only two phases, bcc and liquid. In the ternary Mo-V-C system it has been accepted that V dissolves in the eta MoC phase based on available experimental information. To be able to describe the thermodynamics of the ternary eta phase in the ternary Mo-V-C system it was necessary to treat the thermodynamic properties of the binary metastable eta VC phase. These predictions were based on regularities in bonding properties and vibrational entropy of 3d-transition metal carbides suggested by Fernández Guillermet and Grimvall [39]. In the present work the above estimation procedure have been combined with the CALPHAD method [17, 18], to gain information on the thermodynamics of the metastable eta VC phase which is not known from experiments.

Finally, the ternary interaction parameter in the fcc phase was assessed and thermodynamic calculations in multicomonent model alloys were compared to experimental data with satisfactory results. It was also shown how much this parameter influences the composition in separate phases and also on the amount of different phases in multicomponent systems.

The present author performed the evaluation work and wrote the paper, supervised by Associate Professor Karin Frisk.

6.2 Paper II

A Thermodynamic Assessment of the Co-V System

The binary Co-V system is an important constituent sub-system not only for many high-speed steels and tool steels, but also for cemented carbides. This paper presents a thermodynamic evaluation of the binary Co-V system using thermochemical and phase diagram data, including the magnetic effects due to the behaviour of Co, which is magnetic under 1123 °C. The present work reports the first complete thermodynamic description of the Co-V system. A consistent thermodynamic description, using a Redlich-Kister model [33] for solution phases and sublattice models for the intermetallics, was obtained, and agreed well with the critically evaluated experimental data. The addition of a composition dependent magnetic term led to the prediction of an fcc-Co magnetic miscibility gap, a so-called Nishizawa horn. The ordered hcp phase was modelled using a four-sublattice model and combined with the magnetic description of the fcc phase. This led to that the Co rich region of the phase diagram could be well described. The remaining part of the calculated phase diagram is in satisfactory agreement with experimental information.

The present author performed the evaluation work and wrote the paper, supervised by Professor Bo Sundman.

6.3 Paper III

An Experimental and Theoretical Analysis of the Phase Equilibria in the Fe-Cr-V-C System

The Fe-Cr-V-C system is a critical alloy system for tool steels and high-speed steels due to the very strong carbide-forming elements Cr and V. Knowledge on the phase relations in the Fe-Cr-V-C system, i.e., the relative stability between Cr and V carbides or the solubility of Cr and V in the V- or Cr-rich carbides, is essential for understanding the behaviour of these steels in heat treatments and form the basis for improving the properties or designing new alloys. The old thermodynamic description of this system had some severe drawbacks regarding the phenomena above. Therefore this paper is one of the most important papers in this thesis. New experimental phase equilibria information in the Fe-Cr-V-C system and in commercial alloys are presented and used to modify the thermodynamic description of the system. The main interest was focused on the composition of the MC and M_7C_3 carbides and the necessary adjustment of the Cr and V distribution between carbides and matrix. This has led to a significantly improved description of the distribution of Cr and V in the MC and M_7C_3 carbides. As a result of this improvement the relative stability between the MC carbide and the M_7C_3 carbide also has been improved. Calculations on commercial alloys to verify the new description are presented.

The present author performed the experimental work, did the evaluation and wrote the paper, supervised by Associate Professor Karin Frisk.

6.4 Paper IV

An Experimental Investigation of Carbide/Austenite Equilibria in Commercial Tool Steels and High-Speed Steels Compared Against Thermodynamic Calculations

There exists very little experimental information about the microstructural evolution and composition of the individual phases in tool steels and high-speed steels. When information is available, it can often be doubted whether it has been measured in equilibrium conditions or not. In the present work critical experiments have been performed at 1000 and 1150 °C in order to establish the equilibrium conditions in terms of phase fractions and compositions in three chosen commercial alloys. This information was compared with thermodynamic calculations with Thermo-Calc [16] using two different thermodynamic databases, one old and one new developed by the present work. Using the old database all calculations show the same tendency, the distribution of Cr and V between the matrix and the carbides is inferior, the W and Mo content in the carbides are badly described and the important relative stability between the individual phases is miscalculated. The new database shows much better agreement with the new experimental results.

The present author performed the experimental work, did the calculations and wrote the paper, supervised by Associate Professor Karin Frisk.

6.5 Paper V

Investigation and Modification of Carbide Sub-Systems in the Multicomponent Fe-C-Co-Cr-Mo-Si-V-W System

The recent development of tool steels and high-speed steels has led to a significant increase of the content of Co, Cr, Mo, V and W in the alloys. Therefore the Fe-C-Co-Cr-Mo-Si-V-W system is a very important multicomponent alloy system for these steels. In this paper new experimental information on phase equilibria in the above system and sub-systems are presented and used to modify the thermodynamic description. New experimental data has been obtained both in model alloys and in commercial alloys. The main interest was focused on the composition of the MC, M_7C_3 and M_6C carbides and the necessary adjustment between the carbide-forming elements. The work started by the evaluation of the lower-order systems, Cr-Mo-C and V-W-C, taken higher-order experimental information into consideration, and then finally a reasonable description of the Fe-C-Co-Cr-Mo-Si-V-W system was achieved. Calculations with the new thermodynamic description showed very good agreement with experimental information on model alloys and commercial alloys. The modified thermodynamic description of the Cr-Mo-C and V-W-C, together with all the other earlier investigated important systems, provide a basis for phase diagram calculations of highly alloyed tool steels and high-speed steels over a broad temperature and concentration region, which is very important when developing this type of alloys.

6.6 Paper VI

Diffusion Simulations of MC and M_7C_3 Carbide Coarsening in bcc and fcc Matrix Utilising a New Thermodynamic and Kinetic Description

In this paper the thermodynamic description presented in Paper III was used for all the MC and M_7C_3 carbide coarsening simulations. The new thermodynamic description influences strongly on the coarsening simulations, because the description of the phase stability of the MC and the M_7C_3 carbide has been significantly improved. The kinetic database was revised taking new experimental information on the Fe-Cr-V-C system obtained in this paper, and available experiments on the ternary Fe-Cr-C and Fe-V-C systems, into consideration. The new kinetic description yields an increase of the Cr and V diffusivity in pure fcc Fe with approximately a factor two compared to the old description. Combined with the new thermodynamic description it will affect the rate of coarsening significantly. After the revision the agreement between new experimental results and simulations, both for model alloys and for commercial alloys, was satisfactory. It was found that the interfacial energy of M_7C_3 is twice as large as that of the MC carbide.

The present author performed the experimental work, did the evaluation and wrote the paper, supervised by Professor John Ågren and Associate Professor Karin Frisk.

6.7 Paper VII

Thermodynamic Modelling of the M_6C Carbide in Cemented Carbides and High-Speed Steel

This paper presents an extended thermodynamic description of the M_6C carbide in cemented carbides and high-speed steels. The background of this evaluation is that newly published experimental information on phase equilibria in cemented carbides and high-speed steels have shown that the solubility of Co, Nb, Si, Ta and V in the M_6C carbide is higher than predicted by thermodynamic calculations based on available thermodynamic data. The models are discussed, and the calculated equilibria are compared with new experimental information. Although some approximations in the model have been necessary, due to limited amount of experimental information, a new thermodynamic description has been obtained and gives accurate description of most of the new information.

The present author performed part of the experimental work and did the evaluation involving Si. Also contributed to the writing (background about the model, section 2.1.1, and results and discussion, section 3) and the parts concerning Si.

6.8 Paper VIII

An Investigation of Lower-Order N Containing Systems and New Phase Equilibria Experiments in the Fe-Cr-Mo-V-C-N System

New phase equilibria information in the Fe-Cr-V-C-N and Fe-Cr-Mo-V-C-N systems are presented in this paper. Together with available thermodynamic data in the literature an investigation of lower-order N containing systems have been performed. Most of the nitrogen forms carbonitrides and therefore the elemental distribution dramatically changes when going from MC carbide to a carbonitride. This phenomenon has not been described thermodynamically in a satisfactory way before and is very important for design of new alloys with high nitrogen content. The new thermodynamic description gave results in satisfactory agreement with new experimental measurements as well as with the already existing information. Especially the distribution between Cr and V in the carbonitride has been significantly improved. The results have made it possible to study the substitution of C atoms with N atoms in the carbonitrides through thermodynamic calculations.

All binary and ternary sub-systems containing N have been investigated. For the binary systems only the references are given whereas for the ternary systems the available experimental information is briefly summarised and references are given. Calculated isothermal sections at two different temperatures, using the new thermodynamic description, have been shown for all N containing ternary sub-systems.

The present author performed the experimental work, did the evaluation and wrote the paper, supervised by Associate Professor Karin Frisk.

7. Conclusions and Future Work

7.1 *Conclusions of the work*

Perhaps it is not immediately evident that the new thermodynamic and kinetic databases are the condensed result of a large body of experimental observations. Most of them have been reported previously in the literature and some of them have been made by the present author. It is of course a major challenge to extract something useful and applicable to tool steels and high-speed steels from all this information. The present thesis has shown that computational thermodynamics, i.e. CALPHAD, is an efficient method to handle such a body of experimental information. All the new experimental information has been used to determine thermodynamic interactions in lower-order systems. The lower-order systems have been combined with some quaternary descriptions into a general database for tool steels and high-speed steels.

The new thermodynamic database, TOOL05, has been validated for a number of commercial alloys and makes it possible to predict different thermodynamic properties and phase equilibria with high accuracy. Compared with the old thermodynamic description, the improvements have been significant and the range of applicability has been significantly extended. Reliable results can now be achieved in the composition ranges given in Table 5 and the temperature range 950 °C to 1200 °C.

The adjustments of lower-order systems to reach a satisfactory description when extrapolating up to 8-10 element systems clearly demonstrates the strength of the CALPHAD method. It has also been shown how one can assess tracer diffusion data for mobility evaluation using coarsening experiments combined with the new thermodynamic description.

7.2 *Future Work and Applications*

7.2.1 Extend the Temperature Range

The temperature range needs to be extended to be able to describe the liquidus temperatures, as well as the solidus temperatures in a more satisfying way. However, the more difficult problem is the lower temperatures. The extrapolations down to lower temperatures have not been experimentally verified. The sluggish diffusion at lower temperatures leads to very long equilibration times and one expects that such experimental information are usually not in the equilibrium state. Therefore some critical and well chosen long term heat treatments at lower temperatures should be performed for important systems.

7.2.2 Elements that Needs to be Evaluated and to be Added to the Present Thermodynamic Database

Some of the elements in the present thermodynamic database should be assessed more carefully, e.g. aluminium and niobium. A preliminary investigation has been performed concerning niobium through a diploma work [72] performed at the Corrosion and Metals Research Institute with the author as supervisor. This information is included in the new thermodynamic database and had improved the description of niobium, but more work is needed to be able to reach a satisfactory description of niobium. In particular the effect of niobium together with nitrogen has not been included. Regarding aluminium only available assessments in lower order systems are included. Experience during this work has shown that a deeper investigation is needed to determine the stability between the bcc and fcc phase in alloys containing aluminium.

Other interesting alloy elements to add to the present thermodynamic database are, firstly boron and titanium. Boron acts as a catalyst for nucleation during solidification leading to a finer microstructure whereas titanium is a very strong carbide/carbonitride former. Carbides forming elements frequently used in cemented carbides as e.g. Ta, Zr, and Hf may be interesting for tool steels and high-speed steels in the future. Therefore the future goal is of course to have one large and accurate thermodynamic database which it is able to describe various thermodynamic properties for all these types of materials.

7.2.3 Use of First-principles Calculations

The compound energy formalism [34] and the CALPHAD method [17, 18] need the properties of the end-member compounds. Some of these compounds represent metastable or unstable end-members but must be given proper values to be able to make accurate higher-order extrapolations. Miedema´s formula [40] is one way to give these end-members values and an even better way is to follow the method presented by Fernández Guillermet and Grimvall [39]. The latter approach was used in the present work. However, first-principles calculations might be the best way to describe these end-members nowadays. The research in this field has grown fast and computer development makes it possible to use less severe approximations. First-principles calculations at zero-temperature are nowadays routinely utilised to explain various physical phenomena, and to provide values for various physical properties quantitatively. These different values of different properties can be treated as any other experimental information in the CALPHAD method [17, 18] when evaluating model parameters describing the Gibbs energy of a specific phase under consideration.

The most modern first-principles calculations are based on the celebrated Density-Functional Theory (DFT) and were introduced by Hohenberg and Kohn [73] 1964 and by Kohn and Sham [74] 1965. First-principles calculations have progressed significantly in the last decades. The only information needed to start a calculation is the atomic numbers of the elemental components and initial positions of atoms in the unit cell. First-principles calculations find the electron wavefunction of the structure by minimising its energy solving Schrödinger-like equations. This can be done in many ways as described in a paper by Payne et al. [75]. A ground-state energy of a hypothetic compound and its constituents can be calculated using e.g. the Vienna Ab-initio Simulation Package (VASP) [76, 77].

One aim for the future must be to bridge first-principles calculations and the CALPHAD method [17, 18].

7.2.4 Diffusion Simulations

Further investigation and development of the kinetic description must be performed to be able to treat the nucleation and growth phenomenon in tool steels and high-speed steels in a satisfactory way. The secondary carbides in tool steels and high-speed steels are very important for the mechanical properties. These carbides are formed in the martensitic matrix under the tempering process due to nucleation and growth. Experimental studies of these processes are difficult to perform due to small particle size and theoretical treatments like diffusion simulations are therefore a very powerful tool.

8. Acknowledgements

First I would like to thank my supervisors, Associate Professor Karin Frisk at Corrosion and Metals Research Institute (Kimab) and Professor John Ågren at the Royal Institute of Technology, for lots of stimulating discussions and encouragement, all the help and interest during my work, and also for critical reading of my manuscript.

I would also like to express my sincere gratitude to the following:

- Associate Professor Bo Jansson, Seco Tools AB (at that time at AB Sandvik Coromant), who introduced me during my master thesis to the world of CALPHAD and Thermo-Calc and finally got me interested in a specific field within the broad materials science world.

- The Kimab librarian, Anders Mårtensson, for all the necessary support collecting the many references needed for this thesis, and for locating obscure references and papers published more than 100 years ago.

- To my colleagues at Kimab, Roland Blom and Christer Eggertsson for lots of experimental help, Jacek Komenda for MicroGOP measurements, Ulla Gudmunds Ohlsson for help with the EDS/WDS measurements, Connie Westman for electron microprobe measurements, and Lena Ryde for EBSP measurements.

- To Professor Bo Sundman, Royal Institute of Technology, who I also have shared room with at Kimab, for shearing his enormous knowledge within the field of computational thermodynamics and answering my endless questions about the Thermo-Calc software.

- To Associate Professor Anders Jarfors at Kimab, head of the department, for critical reading of my manuscript and for encouraging me in my work.

- To my colleague Andreas Markström at Kimab, for all the help and comments on present work and the good company.

- To Böhler-Uddeholm AG and Uddeholm Tooling AB, for financial support of the project ’’Thermodynamic databases applied to tool steels and high-speed steels’’ which constitute the basis of this work. I also thank the product development manager at Uddeholm Tooling AB, Odd Sandberg, for great interest and support.

- To Torbjörn Östlund at Kimab, for all the important computer support.

- To Kimab for encouraging postgraduate studies within the framework of research at the institute.

- To my colleagues and former colleagues at Kimab, and the people within the Centre for Computational Thermodynamics (CCT), for providing such a nice working atmosphere, both at the work and outside the work.

- To all of my friends who I spend time with doing many different funny things far away from this topic.

- To my family, which I have been neglecting lately. Thanks for your support and understanding.

9. References

[1] J. W. Langley: Trans ASCE, 27, 1892, pp. 385-405.
[2] A. S. Townsend: Trans ASST, 21, 1933, pp. 769-795.
[3] F. W. Taylor: Trans. ASME, 28, 1907, pp. 31-58.
[4] http://en.wikipedia.org/wiki/Iron
[5] G. Roberts and R. Cary: ''TOOL STEELS – 4th edition'' American Society for Metals, Metals Park, Ohio 44073, 1980.
[6] H. Fischmeister, R. Riedl and S. Karagöz: Metall. Trans. A, 20A, 1989, pp. 2133-2148.
[7] S. Karagöz, R. Riedl, M. R. Gregg and H. Fischmeister: Sonder der praktischen Metallographie, 14, 1983, pp. 369-382.
[8] H. Fredriksson, M. Hillert and M. Nica: Scand. J. Metall., 8, 1979, pp. 115-122.
[9] H. Fischmeister, S. Karagöz and H. O. Andrén: Acta Metall., 36, 1988, pp. 817-825.
[10] J. Bratberg: Zeitschrift für Metallkunde, 96, 2005, pp. 335-344.
[11] K.-D. Löcker, J. Püber, E. Brandstätter and F. Jeglitsch: Härterei-Technische Mitteilungen, 44, 1989, pp. 67-73.
[12] S. Karagöz and H. Fischmeister: Metall. Trans. A, 19A, 1988, pp. 1395-1401.
[13] H. Fischmeister, R.Riedl and S. Karagöz: Metall. Trans. A, 20A, 1989, pp. 2133-2148.
[14] B. Hribernik, G. Hackl, S. Karagöz and H. Fischmeister: Metal Powder Report, 46, 1991, pp. 58-62.
[15] F. Pan, M. Hirohashi, Y. Lu, P. Ding, A. Tang and D. V. Edmonds: Met. Mat. Trans. A, 13A, 2004, pp. 2757-2766.
[16] B. Sundman, B. Jansson and J.-O. Andersson: Calphad, 9, 1985, pp. 153-190.
[17] L. Kaufman and H. Bernstein: ''Computer Calculation of Phase Diagrams with Special Reference to Refractory Metals'', Academic Press, New York, NY, 1970.
[18] N. Saunders and A. P. Miodownik: ''Calphad Calculations of Phase Diagrams'', A Comprehensive Guide, Pergamon Materials Series, Vol. 1, (ed. R. W. Cahn, 1998).
[19] B. Jansson: PhD Thesis, Royal Inst. of Technology, Stockholm, Sweden, 1984.
[20] J. W. Gibbs: Connecticut Academy Transactions, 3, 1875-7, pp. 108-248, pp. 343-524.
[21] J. W. Gibbs: The Scientific Papers of J. Willard Gibbs: Thermodynamics, Ox Bow Press, 1993.
[22] J. Hertz: J. Phase Equilibria, 13, 1992, pp. 450-458.

[23] J. J. Van Laar: Z. Phys. Chem., 63, 1908, pp. 216-253, 64, 1908, pp. 257-297.
[24] J. H. Hildebrand: J. Amer. Chem. Soc., 51, 1929, pp. 66-80.
[25] J. L. Meijering: Philips Res. Rep., 5, 1950, pp. 333-356, 6, 1951, pp. 183-210.
[26] J. L. Meijering and H. K. Hardy: Acta Metall., 4, 1956, pp. 249-256.
[27] J. L. Meijering: Acta Metall., 5, 1957, pp. 257-264.
[28] L. Kaufman and M. Cohen: Prog. Metal Phys., 7, 1958, pp. 165-246.
[29] B. Sundman and J. Ågren: J. Phys. Chem., 42, 1981, pp. 297-301.
[30] M. Hillert and L.-I. Staffansson: Acta Chem. Scand., 24, 1970, pp. 3618-3626.
[31] http://www.thermocalc.se/Products/database_ny/TCFE3.htm
[32] M. Hillert and J. Ågren: ''Diffusion and Equilibria'', Royal Inst. of Technology, Stockholm, Sweden, 1998.
[33] O. Redlich and A. T. Kister: Ind. Eng. Chem., 40, 1948, pp. 345-348.
[34] M. Hillert: J. Alloys Compounds, 320, 2001, pp. 161-176.
[35] P. Gustafson: Met. Mat. Trans. A, 18A, 1987, pp. 175-188.
[36] J.-O. Andersson: Met. Mat. Trans. A, 9A, 1988, pp. 627-636.
[37] G. Inden: Physica, 103B, 1981, pp. 82-100.
[38] M. Hillert and M. Jarl: Calphad, 2, 1978, pp. 227-238.
[39] A. Fernández Guillermet and G. Grimvall: Phys. Rev. B, 40, 1989, pp. 10582-10593.
[40] F. R. de Boer, R. Boom, W. C. Mattens, A. R. Miedema and A. K. Niessen: ''Cohesion in Metals, Transition Metall Alloys'', North Holland, Amsterdam, 1998.
[41] Scientific Group Thermodata Europe (SGTE) Data for pure Elements, Compiled by A. T. Dinsdale, NPL Report DMA(A) 195 (National Physics Laboratory, Teddington, UK, 1989).
[42] W. L. Bragg and E. J. Williams: Proc. Roy. Soc. A145, 1934, pp. 699-730.
[43] A. Kusoffsky, N. Dupin and B. Sundman: Calphad, 25, 2001, pp. 549-565.
[44] N. Dupin: thesis Contribution á l´Evaluation Thermodynamique des Alliges Polyconstitués á base de Nickel, 1995.
[45] B. Sundman, S. G. Fries and W. A. Oates: Calphad, 22, 1998, pp. 335-354.
[46] M. Hillert: Phase Equilibria, phase diagrams and phase transformations, Cambridge 1998, University press.
[47] Y.-M. Muggianu, M. Gambino and J.-P. Bros: J. Chimie Physique, 72, 1975, pp. 83-88.
[48] J.-O. Andersson and J. Ågren: J. Appl. Phys., 72, 1992, pp. 1350-1355.

[49] B. Jönsson: Z. Metallkunde, 85, 1994, pp. 502-509.
[50] J. Kucera and B. Million: Metall. Trans. A, 1A, 1970, pp. 2603-2606.
[51] W. Ostwald: Z. Phys. Chem., 34, 1900, pp. 495-503.
[52] C. Zener: J. Appl. Phys., 20, 1949, pp. 950-953.
[53] G. W. Greenwood: Acta Metall., 4, 1956, pp. 243-248.
[54] I. M. Lifshitz and V. V. Slyozov: J. Phys. Chem. Solids, 19, 1961, pp. 35-50.
[55] C. Wagner: Z. Electrochem., 65, 1961, pp. 581-591.
[56] J.-O. Andersson, L. Höglund, B. Jönsson and J. Ågren: in Fundamentals and Applications of Ternary Diffusion, C.R. Purdy, ed., Pergamon Press, New York, NY, 1990, pp. 153-163.
[57] J. Ågren: J. Phys. Chem. Solids, 43, 1982, pp. 385-391.
[58] A. Bjärbo and M. Hättestrand: Met. Mat. Trans. A, 32A, 2001, pp. 19-27.
[59] J. Ågren: Iron Steel Inst. Jpn. Inst., 32, 1992, pp. 291-296.
[60] G. Carvalho Coelho: Thermodynamik der nioblegierten Schnellarbeitsstähle, Max-Planck-Institute für Metallforschung, Stuttgart, Germany, 1997.
[61] S. Kikuchi: Jpn. J. Phys., 5, 1928, pp. 83-96.
[62] J. A. Venables and C. J. Harland: Phi. Mag., 27, 1973, pp. 1193-1200.
[63] D. J. Dingley: Scanning Electron Microscopy, 2, 1984, pp. 569-575.
[64] B. L. Adams, S. I. Wright and K. Kunze: Metall. Trans. A, 24A, 1993, pp. 819-831.
[65] N. C. Krieger-Lassen, D. Juul and K. Conradsen: Scanning Electron Microscopy, 6, 1992, pp. 115-121.
[66] http://www.abo.fi/fak/mnf/phys.chem/instruments/ripage04.html
[67] M. Ekroth, K. Frisk, B. Jansson and L.F.S. Dumitrescu: Met. Mat. Trans. B, 31B, 2000, pp. 615-619.
[68] http://www.met.kth.se/projects/cct/cct.html
[69] H. Bruce, K. Frisk, U. Gudmunds Ohlsson and A. Markström: IM-Report-2004-514, Stockholm, Sweden, 2004.
[70] D. Turnbull: J. Appl. Physics, 21, 1950, pp. 1022-1028.
[71] M. Y. Wey, T. Sakuma and T. Nishizawa: Transactions of the Japan Inst. of Metals, 22, 1981, pp. 733-742.
[72] S. Canderyd: IM-Report 2005-109, Stockholm, Sweden, 2005.
[73] P. Hohenberg and W. Kohn: Phys. Rev. B, 136, 1964, pp. 864-871.
[74] W. Kohn and L. J. Sham: Phys. Rev. A, 140, 1965, pp. 1133-1138.
[75] M. C. Payne, M. P. Teter, D. C. Allan, T. A. Arias and J. D. Joannopoulos: Rev. of Modern Physics, 64, 1992, pp. 1045-1097.
[76] G. Kresse and J. Furthmueller: Phys. Rev. B, 54, 1996, pp. 11169-11186.

[77] G. Kresse and J. Joubert: Phys. Rev. B, 59, 1999, pp. 1758-1761.